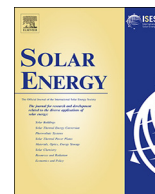




Contents lists available at ScienceDirect

Solar Energy

journal homepage: [www.elsevier.com/locate/solener](http://www.elsevier.com/locate/solener)

## Latent thermal energy storage for solar process heat applications at medium-high temperatures – A review

Alicia Crespo<sup>a,b,\*</sup>, Camila Barreneche<sup>c,d</sup>, Mercedes Ibarra<sup>a</sup>, Werner Platzer<sup>a,b</sup>

<sup>a</sup> Fraunhofer Chile Research – Center for Solar Energy Technologies, Vicuña Mackenna 4860, Santiago, Chile

<sup>b</sup> Faculty of Environment and Natural Resources, Albert-Ludwigs-University Freiburg, Tennenbacher Str. 4, 79106 Freiburg im Breisgau, Germany

<sup>c</sup> Materials Science and Physical-chemistry Department, Universitat de Barcelona, Martí i Franqués 1, 08028 Barcelona, Spain

<sup>d</sup> Birmingham Centre for Energy Storage & School of Chemical Engineering, University of Birmingham, Birmingham B15 2TT, United Kingdom

### ARTICLE INFO

#### Keywords:

Phase change materials  
Thermal industrial processes  
Solar process heat  
Medium-high temperatures

### ABSTRACT

Solar thermal energy has the potential to cover the heat demands of industrial processes. However, there may be a time mismatch between energy supplied by the solar field and the process demand. In this case, a thermal energy storage (TES) allows the use of heat at hours without solar irradiation available. Thermal energy storage for solar hot water or heating systems using low temperatures have been optimized since many decades and are in a mature stage. Developments at high temperatures (above 200 °C) for CSP applications have also been deeply studied. However, until this present paper, limited attention has been paid to TES for solar thermal industrial applications at medium-high temperatures (120–400 °C), where there is a potentially huge demand. When talking about TES several aspects have to be discussed: the heat demand that TES is going to be designed to supply, the material where the energy will be stored and the performance of the TES system which includes not only the material but also tanks, piping and connections.

In this review, food, brewery and chemical industries were identified as the industries with higher potential in which TES and solar energy could be integrated. Heat integration methodologies have been reviewed to optimize the use of the solar energy in the industrial processes.

Regarding the material, latent heat storage or phase change materials (PCM) were selected for this study because they are a very promising type of storage to be integrated in thermal industrial processes, although the state of the art of latent heat thermal energy storage (LHTES) systems is still far from broad commercialization. Until now, no reviews of latent heat storage for industrial applications at medium-high temperatures (120–400 °C) have been published. Therefore, literature related to PCM and latent heat storage (LHS) systems to be used in industrial thermal processes is here reviewed in order to have a general overview of the available technologies for their integration together with solar thermal energy in industrial processes at both experimental and numerical level. More than 100 potential PCMs for heat storage applications in the range of temperatures 120–400 °C have been found. Inorganic eutectic compositions are the group with more potentially available PCM for these applications, with values of heat of fusion between 74 and 535 kJ/kg.

Finally, the works related to the performance of the system from the experimental and modelling point of view were presented. The review of experimental TES systems which include PCM in the studied range of temperatures 120–400 °C showed that most of the experimental set-ups were developed for direct steam generation for CSP applications. Regarding numerical modelling, the type of configuration more simulated is the shell and tube configuration.

### 1. Introduction

Renewable energies, such as solar energy, can substitute or co-work in the energy production to decrease the use of fossils fuels. Solar thermal energy stands as a feasible candidate for obtaining heat for

both industrial and domestic processes. When solar energy is used, the discontinuity of the sun irradiation could cause a heat supply disruption. Thermal energy storage (TES) reduces this time mismatch between energy supply and demand, increasing the reliability of solar thermal systems. The heat that is not required by the process during sun hours

\* Corresponding author at: Fraunhofer Chile Research – Center for Solar Energy Technologies, Vicuña Mackenna 4860, Santiago, Chile.

E-mail address: [alicia.crespo@fraunhofer.cl](mailto:alicia.crespo@fraunhofer.cl) (A. Crespo).

<https://doi.org/10.1016/j.solener.2018.06.101>

Received 31 October 2017; Received in revised form 17 April 2018; Accepted 25 June 2018

0038-092X/ © 2018 Elsevier Ltd. All rights reserved.

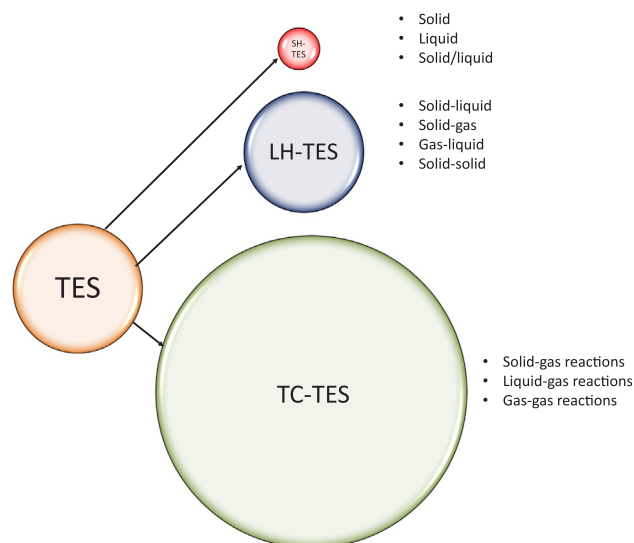


Fig. 1. TES methods and the scheme of TES heat storage capacity of each one.

can be stored to be later used when there is no solar irradiation.

Thermal energy storage (TES) has been commercially used in solar thermal applications since more than 20 years, mainly for low-temperature solar domestic hot-water and heating systems, but in the last years also for large concentrated solar power (CSP) plants operating at temperatures up to 560 °C, in order to provide them independence from the sun. Thermal energy storage systems (TESS) can be classified by the method used to store the heat: Sensible heat thermal energy storage (SHTES), latent heat thermal energy storage (LHTES) and thermochemical thermal energy storage (TCTES). SHTES is the simplest method to implement TESS but the heat amount of energy able to store by this method is the lowest as is represented in Fig. 1. LHTES is able to store 3–4 time more than SHTES and although this method is commercially implemented, LHTES systems present highest technical risk. Moreover, TCTES is the most promising TES method but the technical barriers make this technology not completely full-implemented in the market. In Fig. 1 the heat storage capacity of these three technologies is shown. The use of one type or the other will depend on the application in particular.

This paper focuses on applications for industrial heat demand at medium-high temperatures (120–400 °C), which covers around 19% of the EU-27 industrial heat demand (Krummenacher and Muster, 2015). Until now little attention has been paid for TES integration at those applications. The integration of solar thermal technologies with TES in industrial processes could reduce the amount of used fossil fuel, reducing CO<sub>2</sub> emissions. The use of heat integration methodologies may help to optimize the size and integration points for the best energy efficiency of the system. However, industries usually have a problem with the integration of solar thermal energy together with thermal storage because of the large amount of required space. PCM could solve the space problem at the same time than can provide heat at a nearly constant temperature, which is necessary for some thermal industrial applications at medium-high temperatures. Therefore, LHTES are the selected TES for this study.

A considerable amount of reviews which include latent heat storage materials and systems for different temperatures and applications have been published. Several of them deal with LHTES for CSP applications. Gil et al. (2010) and Medrano et al. (2010) presented reviews of the different storage concepts and storage materials (SHTES, LHTES and TCTES) for high temperature CSP applications. Cárdenas and León (2013) and Liu et al. (2012) reviewed LHTES for solar applications above 300 °C. Kenisarin (2010) presented a review of PCM for solar applications with a range of temperatures of 120–1000 °C, where the thermophysical properties of potential materials like salt compositions

and metal alloys were also presented. Zalba et al. (2003) published a review of solid-liquid phase change materials focused on materials, heat transfer and applications. Furthermore, several reviews about solar cooling applications have been presented, most of them reviewed latent heat storage below 150 °C (Brancato et al., 2017; Khan et al., 2017), except Pintaldi et al. (2015), whose review of LHTES media and systems reached PCM with melting temperatures up to 250 °C. Moreover, reviews of PCM for solar heating applications (Mahfuz et al., 2014), solar water tanks with PCM layers (Jabbar et al., 2013) or solar water heating systems with PCM floor (Huang et al., 2014) at temperatures below 100 °C have been published. Reviews of PCM used in buildings (Cabeza et al., 2011) or for automotive applications (Jaguemont et al., 2018) have been also performed.

Although, a lot of information is available, LHTES storage concepts and materials for CSP, cooling or heating applications are in many cases not suitable with industrial applications because of the range of temperatures and of the requirements of the process itself. Until now no reviews of LHTES for medium-high temperatures (120–400 °C), focused on industrial applications, have been published.

Therefore, the objective of this paper is to gather information related to TES systems applied to medium-high temperatures (120–400 °C) industrial applications. Several aspects are discussed in the following sections: the heat demand that TES is going to be designed to supply, the material where the energy will be stored and the performance of the TES system. In Section 2, potential industries in which TES and solar energy could be integrated were identified as well as heat integration methodologies for a maximum utilization of solar and TES systems. Regarding the material, latent heat storage materials or phase change materials (PCM) were selected since they have higher heat storage densities compared to sensible ones. Furthermore, they can provide heat at a nearly constant temperature. Therefore, Section 3 focuses on PCM materials available up to the publication of this work. In Section 4, experimental and numerical systems which include PCM in a range of temperatures at 120–400 °C were identified, in order to get a general overview of available technologies for their integration together with solar thermal energy in industrial processes at both experimental and numerical level. Enhancement techniques have been also included in this section. Finally, the conclusions are presented in Section 5.

## 2. Integration of solar process heat at medium-high temperatures for industrial processes

Identifying and characterizing the heat demand that TES will have to cover is an important step when analyzing the suitability of a TES system. Hence, in this section the potential industries whose demand could be covered by a solar thermal and TES system are identified, the different kind of TES integration schemes are described and the heat integration methodologies for the correct design are evaluated.

### 2.1. Identification of potential industries to integrate solar process heat

Thermal energy storage systems are required for solar thermal applications because of the discontinuous nature of the irradiance of the sun. If solar heat were to cover the thermal demands of an industry that needs heat when there is no solar irradiation, thermal energy storage systems are required. Therefore, the objective of this section is to identify the industries whose demands are more suitable for the integration of solar thermal energy and thermal energy storage (TES).

The potential to meet the thermal energy demands with solar energy has been studied on several occasions. Schweiger et al. (2000) made a study of the potential of solar heat in industrial processes in Spain and Portugal. They also summarized different analysis of industrial heat demand for several countries around the world (U.S.A, Switzerland, Germany, U.K, Japan, Portugal and Spain). They concluded that 15% of the total energy demand in Europe was industrial heat demand. All of

their analysis agree that more than 50% of the total industrial demand was in the range of temperatures below 250 °C. According to these authors, the following industries have a high fraction of heat demand being good options to introduce solar energy at medium temperatures: food industry (66%), chemical industry (58%) and textile industry (30%). In particular, the following processes were identified as good candidates: refrigeration for brewing purposes, sterilization for milk industry (130–150 °C), drying processes for textile industry (140–220 °C) and paper industry (~180 °C). Kalogirou (2003) made a study of the potential of solar industrial process heat applications in Cyprus. The authors identified several industries with suitable conditions for the coupling of solar energy into their processes. Again, food industries, especially milk and meat industries and breweries, were identified as the ones with the greater potential for solar heat integration.

Vannoni et al. (2008) showed the results of ECOHEATCOOL project in which an analysis on the heat demand in industrial sectors of 32 countries (EU25 + Bulgaria, Romania, Turkey, Croatia, Iceland, Norway and Switzerland) was performed. The report showed that 30% of the industrial heat demand is below 100 °C, 27% is at medium temperatures (100–400 °C) and 43% at high temperatures (over 400 °C). Fig. 2 (Solar Heat for Industry – Solar Payback, 2017) shows similar percentages of heat demand in the world. The report of the Task 49 of IEA Solar Heat and Cooling (Krummenacher and Muster, 2015) fixed industrial heat demand at medium temperature (100–400 °C) in 19% of the total heat demand. According to this same report, the highest demands at medium temperature were in the chemical, food, drink, tobacco and paper industry.

Kurup and Turchi (2015) made also an assessment about the potential integration of concentrated (Parabolic Trough Collectors and Linear Fresnel) solar heat in industrial processes, in this case for the state of California. The authors defined the heat transfer fluid (HTF), the temperature range and the collector technology more suitable for each application (Table 1). They concluded that the most common range of temperatures of the steam industrial demand was between 120 and 220 °C, and usually below 260 °C. The five industries identified by the authors based on previous research, which used more steam at less than 260 °C were food, paper, petroleum, chemicals and primary metals. That selection of industries agrees with the results from other reports or publications.

All the mentioned studies had in common that a high heat demand in industry is in the range of temperatures between 120 and 260 °C and that the industries with more potential to introduce solar thermal energy are food and chemical industries. Parabolic trough and Fresnel collector technologies combined with thermal oil as HTF can reach until 400 °C. Furthermore, the Task 49 of IEA Solar Heat and Cooling (IEA/SHC) (Krummenacher and Muster, 2015), which covers solar heat integration for industrial processes, includes the thermal processes in a

**Table 1**  
Temperature regions relevant for solar process heat integration (Kurup and Turchi, 2015).

Temperature range	Solar collector type	HTF	Applications
< 80 °C	Flat plate Non-tracking compound parabolic Solar pond	Water	Hot water Space heating
80–200 °C	Parabolic trough Linear Fresnel	Water/steam	Hot water or steam for IPH (Industrial Process Heat)
200–300 °C	Parabolic trough Linear Fresnel	Mineral oil	Steam for IPH
300–400 °C	Parabolic trough Linear Fresnel	Synthetic oil	Steam for IPH
400–550 °C	Parabolic trough Linear Fresnel	Steam or molten salts	Electric power
> 550 °C	Heliostat/central receiver Parabolic dish	Steam or molten salts	Electric power

temperature range up to 400 °C. Since a high heat demand exists for medium-high temperatures (120–400 °C) in industry and until now few attention have been paid to those temperatures, especially regarding the integration of latent heat thermal storage, this study focus in the just mentioned range of temperatures (120–400 °C).

The costs of the solar thermal field have direct influence on the integration of thermal energy storage in industry. If the prices of the solar thermal field are too high, it will be discarded as a heat source, since it is easier to use a gas boiler when heat is required. Kurup and Turchi (2015) paid attention to the costs and concluded that the cost of an installed SIPH (solar industrial process heat) plant based on developer information is about 200 US\$/m<sup>2</sup> considering PTC and linear Fresnel systems. Depending on the irradiation resource of the location and the price of natural gas, the use of solar thermal energy to cover the industry demand could be or not economically feasible.

A Technical Study Report of Solar Heat for Industrial Processes (Cottret and Menichetti) presented the costs of a solar thermal process heat installation in Europe, which were in a range between 180 and 500 €/m<sup>2</sup>. This range of cost was wide since several factors influenced on it, such as the solar fraction, climatic conditions, system design and type of technology. In the same report, the cost distribution for a large scale solar thermal plant was presented. This corresponded mainly to the collector field (48.4%), piping (18.8%), planning (14%) and buffer storage and heat exchanger (11.4%).

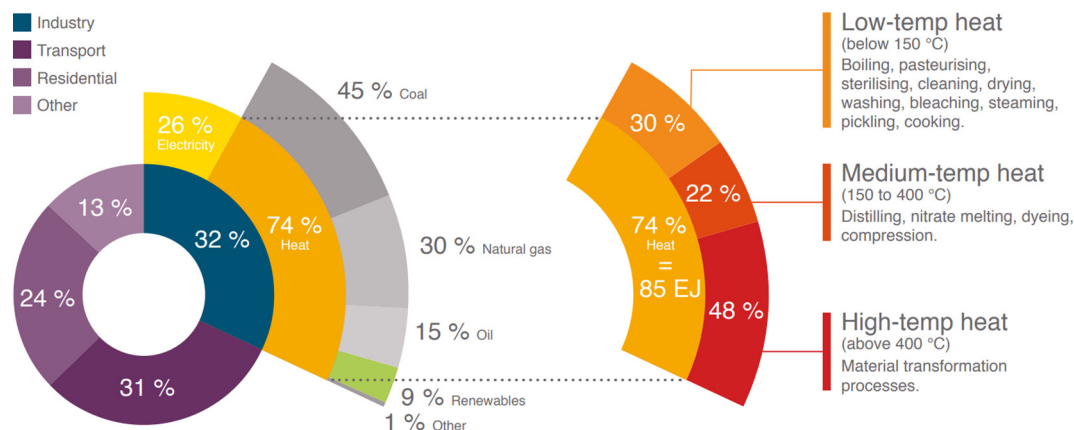


**Fig. 2.** Total final energy consumption 2014: 360 Exajoule (Solar Heat for Industry – Solar Payback, 2017).

## 2.2. Types of thermal energy storage systems (TESS)

As Heller (2013) and Gil et al. (2010) summarized, there are three types of TESS. The TESS are classified in active and passive. An active storage system is mainly characterized by forced convection heat transfer into the storage material (Gil et al., 2010). An active system is subdivided into active direct and active indirect systems. In a passive storage system, the storage material doesn't flow through the system, but is the HTF which flows through the storage material for charging and also for discharging. The TESS classification is shown below.

**Active direct storage systems:** in this type of system, the heat transfer fluid from the solar collectors and heat storage material are the same. This arrangement can be used in CSP plants with sensible heat materials (usually synthetic oils or molten salts). These sensible heat materials are suitable for CSP plants because they stay liquid at the temperatures required to produce electricity in Rankine cycles. Water at low temperatures is also usually stored using an active direct storage systems in both industrial and residential applications. Materials used in active direct storage systems must fulfil the requirements of both a heat transfer fluid (HTF) and the storage material.

From an economic point of view, with active direct storage systems large heat-exchangers are not required, which decreases the equipment costs. On the other hand, if molten salts are considered, they have a high price and they may need an auxiliary heater to avoid them to freeze below 120–220 °C depending on the material. This kind of storage is non-viable when Direct Steam Generation (DSG) plants are considered or when the HTF is gas. The reason is that either very large storage tanks would be required or storage tanks with high pressure, which would increase the tanks cost and would make the maintenance more complex.

One active direct storage system example is an arrangement with 2 tanks (Fig. 3). One tank contains the hot HTF/storage material and the other the cold HTF/storage material. Hot HTF is stored in the hot tank until it is required, flowing to the heat exchanger of the Rankine cycle and being afterwards stored once it was cool down in the cold tank. Cold HTF/storage material will be again recirculated through the solar field absorbing heat, the cycle starts again.

**Active indirect storage system:** in this kind of arrangement, the heat transfer fluid and the storage material are different. A heat exchanger is required to perform the heat exchange between the

materials. There are two types of these systems, one is with two tanks, which works like the active direct system, but in this case the heat is stored in a different material (generally molten salt) to the HTF (generally oil). An oil-molten salt heat exchanger is required for the charging and discharging cycles of the storage system. In Fig. 4, an active indirect storage system with two tanks is shown. The other type is with only one tank, called thermocline. In the thermocline tank, the hot and cold storage materials are separated via stratification. Depending on the cost of the storage fluid, the thermocline can result in a substantially low cost storage system (Gil et al., 2010). Although having an active storage system of a latent heat storage material is not common, a publication about an experimental demonstration of a novel active latent heat storage system has been recently published (Pointner and Steinmann, 2016).

**Passive storage system:** it consists of a solid material through which the HTF passes for charging and again for discharging. Fig. 5 shows a CSP plant with a passive storage system. The disadvantage of this kind of systems is that during the discharging process, the temperature of the HTF decreases because the storage material is cold down. Furthermore, the heat transfer is low (Gil et al., 2010). Phase Change Materials tend to be used as storage material for passive storage system. The melting temperature of the PCM must be the same as the charging/discharging temperature of the HTF in order for the heat-exchange to occur. Other materials, such as concrete or rocks which use sensible heat are used also in passive storage systems.

## 2.3. Solar heat and TES integration methodologies in industry

In the last years, the number of publications regarding heat integration methodologies using solar heat as hot utility in industrial processes has increased, most of them for low-medium temperature processes. Heat integration methodologies are crucial for the success of solar heat and thermal storage integration in thermal industrial processes. These methodologies allow the increase of the energy efficiency of thermal industrial processes due to the use of waste heat, optimization of the water/steam network design and thermal energy storage.

Pinch Analysis (PA) is a widely used methodology for the assessment of heat recovery potential of an industrial process and for the design of the thermal network. To apply PA approach, heating and cooling demand for the processes is required. PA allows to obtain the

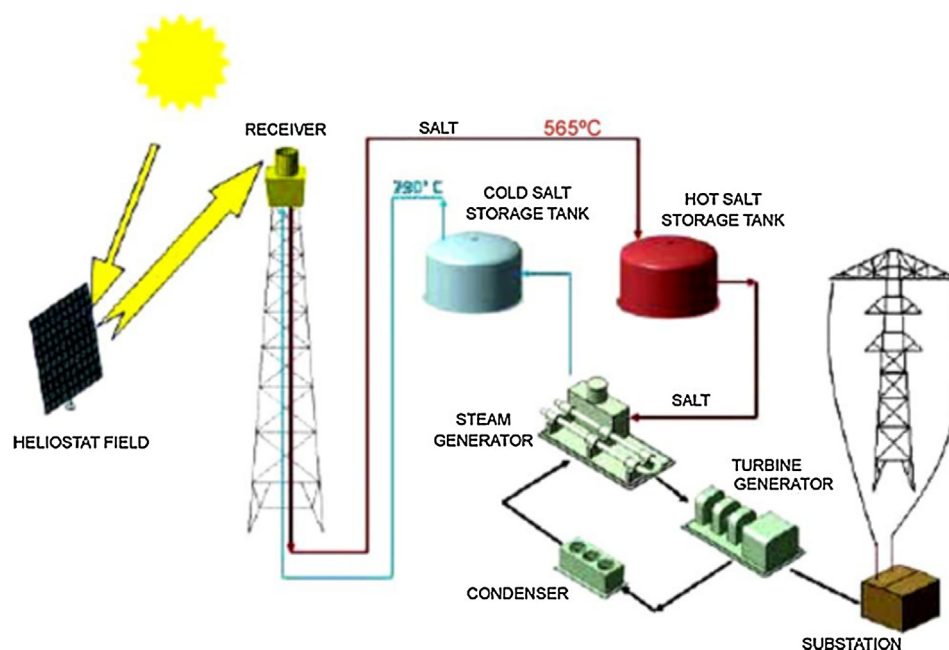


Fig. 3. Scheme of Gemasolar CSP Plant with an active direct storage configuration with two tanks (Plataforma Solar de Almería. Informe Anual, 2007).

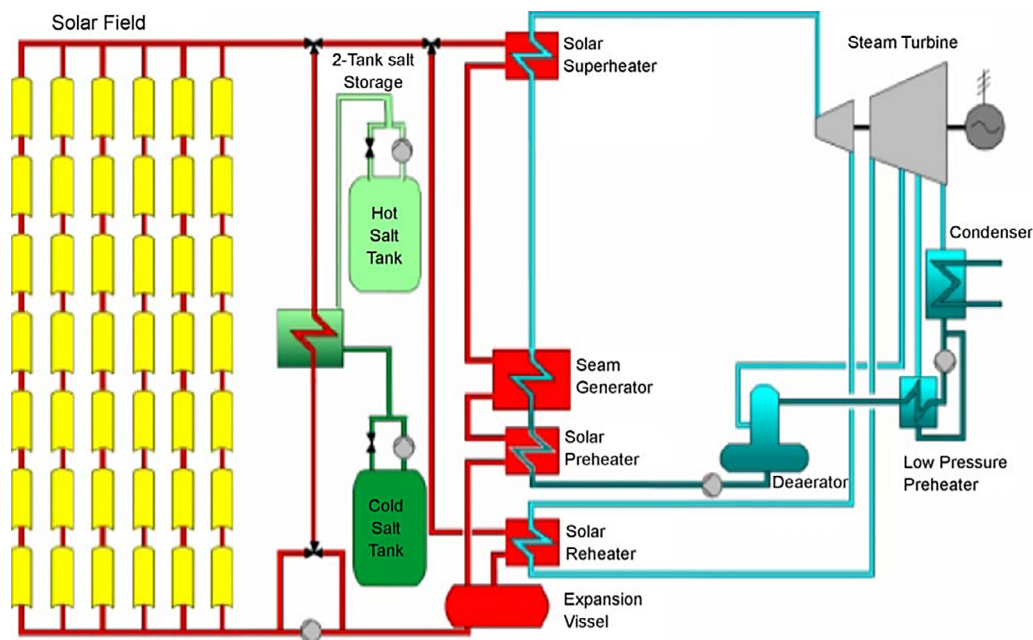


Fig. 4. Active indirect storage with two tanks (Herrmann et al., 2002).

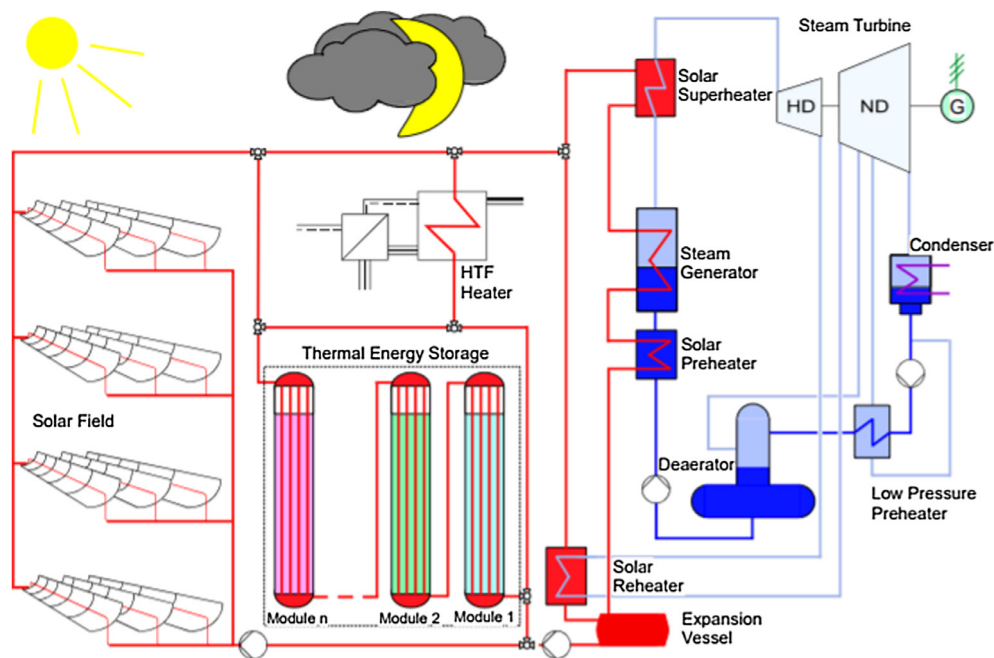


Fig. 5. CSP Plant with PCM passive storage system (Herrmann et al., 2002).

maximum heat recovery of a process through the drawing of the so-called Composite Curves (CC) and also allows to identify the most efficient energy supply through the drawing of the so-called Grand Composite Curves (GCC). In the CC, the temperature enthalpy profiles of hot and cold streams are drawn. The GCC derives from CC and represents the temperature profile of the remaining heating or cooling requirements (Muster et al., 2015). Another important parameter of PA is  $\Delta T_{\min}$ , which is an economic parameter representing the optimal trade-off between energy savings and capital costs (Muster et al., 2015). In the following paragraphs, it is noted that various authors based their solar heat and thermal storage integration methodologies on Pinch Analysis.

Heat integration methodologies, such as PA, can be applied for continuous or batch processes. Because of the discontinuity of the

demand over the time and of the heat sources, (in case of the sun) specific heat integration methodologies for non-continuous processes must be developed. The discontinuity of demand and source over the time causes a higher level of difficulty to develop these methodologies. One option to assess batch processes is to apply the Time Average Model (TAM). The TAM is a method where Pinch Analysis is applied to batch processes. It considers an average value of the heat load over time. In these processes, hot and cold utilities are normally not coincident in time, and therefore it is not possible to exchange heat between utilities. Another method to assess batch processes is the Time Slice Model (TSM) (Kemp, 2007). In this method the batch cycles are divided into several time intervals and one minimum temperature difference ( $\Delta T_{\min}$ ) is calculated for each time interval, instead of calculating one  $\Delta T_{\min}$  for all the streams. Under these conditions opportunities for

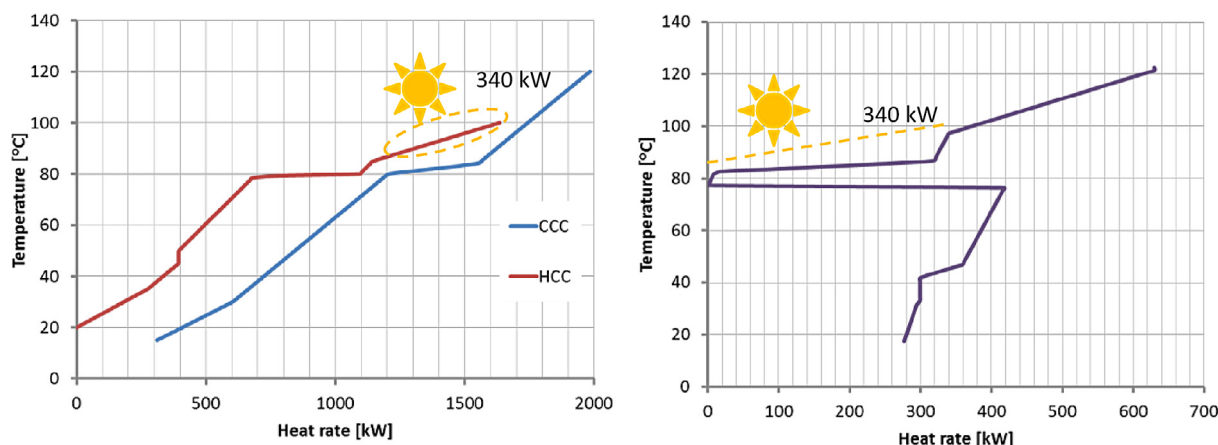


Fig. 6. CC including solar heat as a hot utility stream; GCC including heat recovery options,  $\Delta T_{\min} = 5^\circ\text{C}$ ; (CCC: cold CC; HCC: hot CC) (Muster et al., 2015).

maximum energy recovery can be obtained for batch processes.

Some authors studied the integration of solar heat in thermal industrial processes without the incorporation of TES. Some of them have done it through Pinch Analysis, which is a suitable tool to identify the energy saving potential of solar heat in thermal industrial processes. In Fig. 6, the Composite Curves with the integration of solar heat as a hot utility are shown. Atkins et al. (2010) presented the integration of solar thermal in low-temperature-pinch batch dairy plant. They concluded that the thermo-solar system had to be placed as a hot utility source above the pinch point. Quijera et al. (2011) used Pinch Analysis to assess the viability of the integration of solar thermal energy in a dairy plant at low-medium temperatures that were required by different batch processes. They concluded that solar heat could be considered as a potential hot utility. Some years later, Quijera et al. (2013) developed a methodology based not only on Pinch Analysis, but also on exergy analysis to evaluate different approaches of solar heat integration for a particular batch industrial process. The authors described the combined methodology as very powerful for the energy optimization and optimal integration purpose. Recently, Eiholzer et al. (2017) presented a methodology based on pinch analysis to optimize a low-temperature batch industrial process (brewery) and to integrate a solar thermal system. The time average model (TAM) and time slice model (TSM) were used to obtain the heat recovery objectives. Comparing the heat recovery potentials of the TAM and TSM, the authors concluded that indirect heat recovery by thermal energy storage is essential to reduce the energy demand of the brewing process.

Some authors have developed methodologies to integrate both solar heat and thermal storage in thermal industrial processes. Walmsley et al. (2014) integrated solar heat through the Heat Recovery Loops (HRL) method based on constant (CTS) and variable temperature storage (VTS) in an industrial activity. This industrial activity consisted of an inter-plant formed by semi-continuous processes. The Heat Recovery Loops method is a pinch based method to transfer indirectly heat from one process to another using a heat transfer fluid and thermal storage. According to the authors, the storage system influences in the construction of the Composite Curves (CC). Moreover, the shape of the CC together with the pinch temperature influence on how solar heating is integrated. For their case study, the VTS approach achieved 37% of heat recovery more than the CTS case. Furthermore, they concluded that solar heat could be integrated directly as a hot utility in the HRL if the system had a pinch around the cold storage tank temperature.

Muster et al. (2015) presented, in the frame of IEA/SHC Task 49, a methodology for obtaining the most adequate integration points of solar heat using also thermal energy storage in the heat exchange network of industrial processes. The authors proposed a methodology for solar heat integration that included three main parts: 1. Pre-feasibility, 2. Feasibility study, 3. Decision making and detailed plan. Fig. 7

shows possible integration points for process heat storage (Muster et al., 2015). The integration options identified in the report were: i. Solar energy storage (store in primary circuit), ii. Process heat storage (unit B3 -store in secondary circuit) and iii. Supply heat storage (unit A2 -store in secondary circuit). In another report of IEA/SHC Task 49 (Krummenacher and Muster, 2015), a fourth integration option is showed (Fig. 8). The figure shows the integration of a single-combined storage tank in a solar powered-thermal process. In this case, the whole thermal network shared only one storage tank with different temperature levels.

Besides the studies of Task 49 IEA/SHC (Krummenacher and Muster, 2015; Muster et al., 2015); Krummenacher and Favrat (2001) presented a methodology for the heat integration in industrial batch processes that dealt also with thermal storage integration. The methodology defined the minimum number of heat storage units based on Pinch Analysis (PA).

Other authors have considered methodologies for thermal energy storage integration in industrial processes. In these approaches, solar heat was not taken into account as a hot utility, but the methodologies could be applicable for it too. Atkins et al. (2010) studied the potential for low-temperature indirect heat transfer between plants using the heat recovery loop (HRL) approach and a stratified tank in a dairy factory. They came to the conclusion that the maximum amount of heat recovery could be increased if the temperature of the hot fluid in the recirculation loop was varied depending on which condition the site was operating under. Atkins et al. (2012) continued with this study in a new publication, where they concluded that both the HRL temperature range and a small heat storage volume could considerably enhance the amount of heat recovery. They highlighted the importance of the control system for a good performance of the system.

Walmsley et al. (2012) studied different approaches of heat exchanger area targeting and storage temperature selection for Heat Recovery Loops for a maximum heat recovery. They performed a comparison between a methodology based on  $\Delta T_{\min}$  approach (PA) with three global optimization approaches with different constrains (same Number of Heat Transfer Units, Log-Mean Temperature Difference and no constraints). They concluded that the  $\Delta T_{\min}$  approach was efficient for HRL design compared to other methods which needed high amounts of computational calculations. Moreover, optimizing the selection of the storage temperatures was worthwhile and allowed the minimization of the heat exchanger area.

Other energy targeting approach with thermal storage is the Cascade Analysis, which allows heat to be cascaded with respect to time and temperature (Klimes, 2013). This methodology also allows the identification of the heat storage opportunities for batch processes. It was Kemp and Deakin (Kemp and Deakin, 1989) who presented a methodology based on Cascade Analysis, which showed what storage

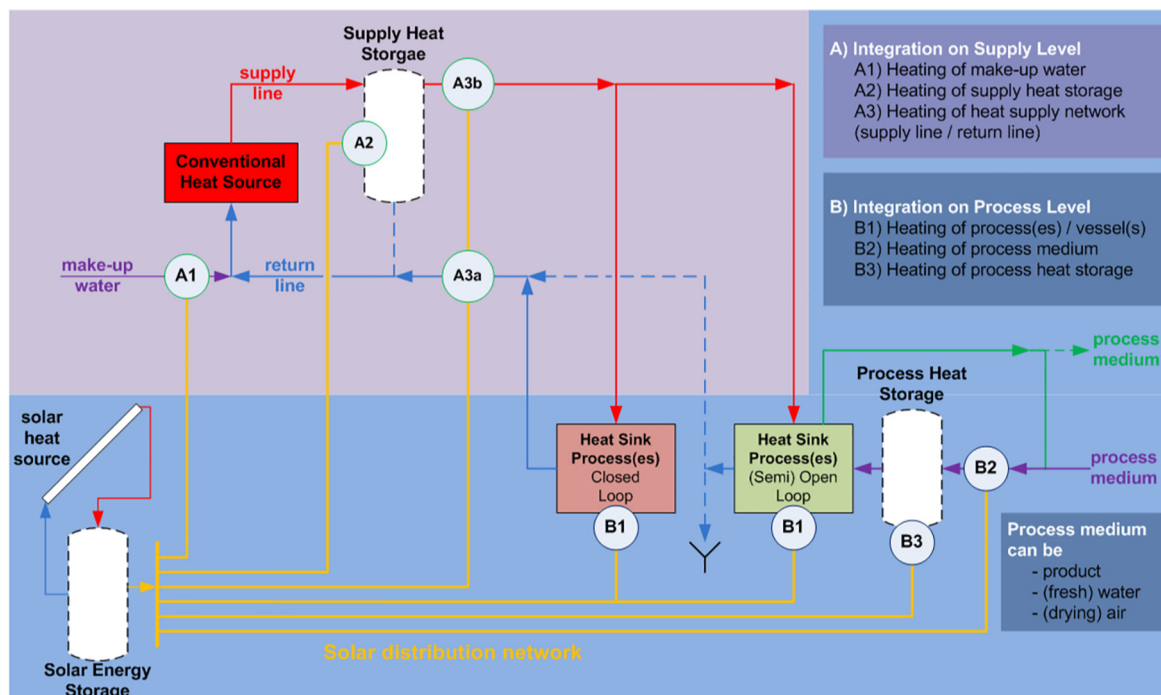


Fig. 7. Possible integration points for solar process heat (Muster et al., 2015).

times and temperatures were needed to reach the Time Average Model approach (TAM) (Linnhoff et al., 1988). However, the algorithm is complicated and has not been commercially used. Furthermore, the cascade analysis was found not to be rigorous with the heat storage capacity (Klemes, 2013).

In contrast with most of the heat integration methodologies, which are based on PA, Chen and Ciou (2009) presented a method for heat recovery systems for batch processes which is not based on Pinch Analysis, but in mixed-integer nonlinear program (MINLP) and an iterative method. They presented an iterative method for designing indirect heat recovery system in batch plants using a recirculated HTF and the integration of a variable-temperature/variable mass storage (VTVM). To reduce the number of external utilities, they used of a

mixed-integer nonlinear program (MINLP). In order to assess the non-linearity of the temperature profile in the VTVM system an iterative method was presented. This method, already demonstrated, linked a network optimization tool (a General Algebraic Modeling System or GAMS program) for network design and a MATLAB program for storage temperature simulation. According to Chen and Ciou (2009) the size of VTVM storage would be smaller than that of the fix temperature/variable mass.

In conclusion, the integration concepts for solar process heat into industrial processes using thermal energy storage working at medium-high temperatures is a field where a lot of research still needs to be carried out in order to use as much solar energy as possible and to reduce the total amount of consumed energy. Few reduced amount of

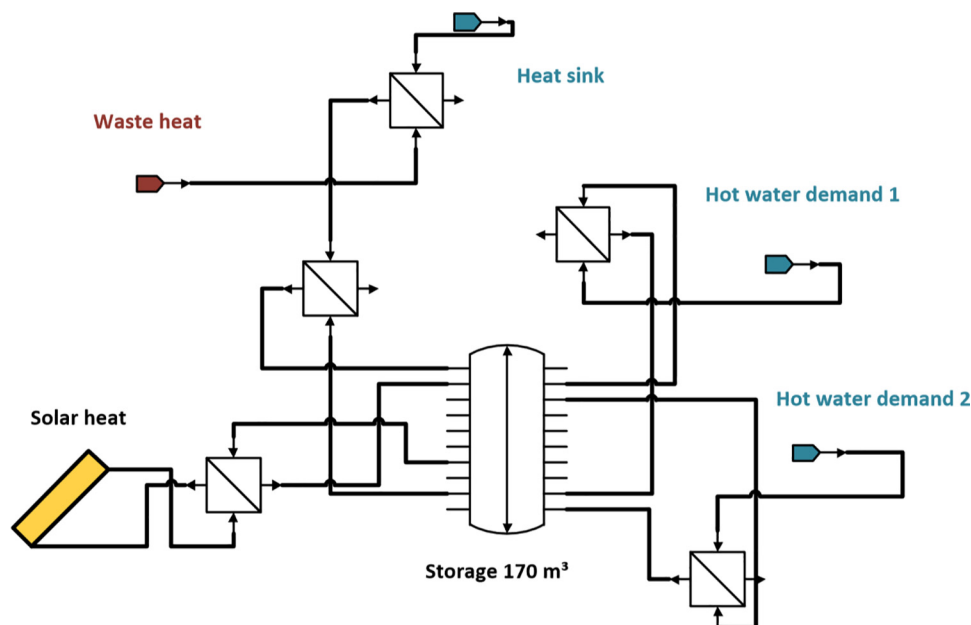


Fig. 8. Heat integration with solar heat + combined storage (Krummenacher and Muster, 2015).

publications dealt with the integration points of TES for Solar Heat Industrial Plants (SHIP), but state-of the art publications on methodologies for solar heat and thermal energy storage integration have been presented. This topic is a key research area for the proper integration of solar thermal energy in industrial applications. New storage management tools and optimized algorithms should be developed in order to integrate TESS and obtain more energy efficient processes.

Further investigation of the influence of different temporal load profiles is necessary because the match between heat demand loads and possibilities for heat recovery has a large impact on the integration of solar systems (Lauterbach et al., 2014). If demand and generation profiles do not match, storage solutions could provide a possibility to improve the coverage of the demand and hence of the overall efficiency. Especially in batch processes, the possibility to store energy for a certain time presents a large potential for improvement. In this case, LHTESS provides a thermodynamically ideal possibility to store isothermally heat at the melting temperature of the PCM. Furthermore, PCM have a higher storage density compared to sensible TES which reduces the size of the storage tank.

### 3. Latent heat materials at medium-high temperatures

Latent heat thermal storage materials are selected for the present review because of their isothermal phase change and their high storage density. Although some experimental studies of PCM in the range of temperatures of the present review have been recently performed (Pollerberg et al., 2012; Bhale et al., 2015; Garcia et al., 2015; Joemann et al., 2016; Bayón et al., 2010; Willwerth et al., 2017; Johnson et al., 2014), latent thermal energy storage systems at medium-high temperatures have barely been used in industry.

#### 3.1. Latent heat

Latent heat of a material is the heat that carries a phase change of the material, with no change in the chemical composition. Latent heat transfer happens at constant temperature, property which makes latent heat materials good allies for certain applications. This constant temperature is the melting temperature of the material. Furthermore, usually latent heat materials have a higher heat storage density compared to sensible heat ones. Therefore latent heat materials need less space to store the same amount of energy. The latent heat transfer of a material is equal to its variation of enthalpy ( $\Delta H$ ) between the two different phases (Eq. (3.1)).

$$\Delta Q = \Delta H \quad (3.1)$$

For industrial purposes, space plays an important role, especially in industries that are in urban areas. Hence, PCM are a potential solution to store energy in relatively small volume. There are three different types of latent heat depending on the type of phase change of the material: solid-liquid, solid-solid and liquid-vapor. The materials in solid-liquid phase change which can be used for heat storage are called phase change materials (PCM). Solid-solid latent heat materials which can be used for heat storage, are also considered Phase Change Materials.

#### 3.2. PCM classification

##### 3.2.1. According phase change

###### Latent heat of solid-liquid phase change

This type of latent heat materials is based on melting and solidification processes and it allows storing large amounts of heat in a smaller volume compared to sensible heat materials. During melting, the temperature stays constant (see Fig. 9) in the so-called melting temperature or phase change temperature. Once the melting process is finished, further transfer of heat will happen through sensible heat storage (Cabeza and Mehling, 2008). The heat transfer during the melting or

phase change, which cannot be measured via temperature change (temperature is constant) is called latent heat and can be measured via the enthalpy difference between the two phases as was mentioned before. The difference of enthalpy in the case of solid-liquid phase change is called phase change enthalpy, melting enthalpy or heat of fusion. However, one issue to consider with phase change materials is the volume change after the phase change. Usually the liquid phase needs a larger space to be contained. If the container is big enough to fit the phase with larger volume that means that the pressure will stay almost constant during the phase change. Therefore, the heat transfer process (melting and solidification) will occur at constant temperature.

###### Latent heat of solid-solid phase change

Solid-solid phase change materials (SSPCM) have the advantage over solid-liquid PCM that they do not have to be encapsulated because there are no leakage issues, which may make systems cheaper. Moreover, solid-solid PCM are simple and easy to handle. However, the heat of phase change of SSPCM is lower than for the solid-liquid PCM. This disadvantage has to be overcome in order to use them for commercial applications.

###### Latent heat of liquid-vapor phase change

In this type of latent heat the liquid-vapor phase change happens through the evaporation and condensation processes allowing the storage of latent heat. The much larger volume of the vapor phase compared with the liquid one causes some disadvantages which make from this kind of material unsuitable for thermal storage. In a liquid-vapor phase change, the phase change temperature strongly depends on the boundary conditions, and therefore the phase change is not just used for storage of heat alone (Cabeza and Mehling, 2008). Because of the volume increased in the vapor phase, the tank would have either to support very high pressure or have a very large volume. Therefore, they are not used as latent heat storage materials. If the material would be without container that means that the material will be wasted and would cause environmental impact (except for water).

##### 3.2.2. According composition

There are three types of solid-liquid phase change materials relevant for heat storage applications: organic, inorganic and eutectic materials. Advantages and disadvantages of phase change material are presented here. A schematic summary of the properties of PCM is presented in Fig. 10.

Organic liquid-solid PCM are classified between paraffin and non-paraffin. Paraffin have several advantages like being cheaper than other PCM, having low vapor pressure, high heats of fusion and chemical stability (Khan et al., 2017; Sharma and Sagara, 2013). Moreover, they are compatible with all metal containers, although attention must be taken when a plastic container is used (Sharma and Sagara, 2013). They also have some disadvantages such as low thermal conductivity and high-volume change with phase change.

Non-paraffin is the largest category for potential use as latent heat storage materials (Sharma and Sagara, 2013). They have general advantages, such as having little subcooling and thermal and chemical stability and the disadvantage of having low thermal conductivity. Paraffins tend to have all similar properties, however non-paraffin have different properties based on each material (Sharma and Sagara, 2013). Further properties of paraffin and non-paraffin are listed in the Table 2. Non-paraffin are divided into fatty acids, alcohols, esters and glycols. Fatty acids have similar features as paraffin (Sharma and Sagara, 2013). However, they are much expensive.

Inorganic PCMs are the second type of PCM. They have advantages like high enthalpy and higher thermal conductivity than organic PCMs (Khan et al., 2017). Salts, salt hydrates, hydroxides, metals and metal alloys are different types of inorganic PCMs. Low melting point metals and their alloys have the ability of high thermal conductivity and small volume change, therefore they could potentially be a good material. However, they have low heat of fusion per unit weight (Ge et al., 2013), which means that a higher volume is required for a certain amount of

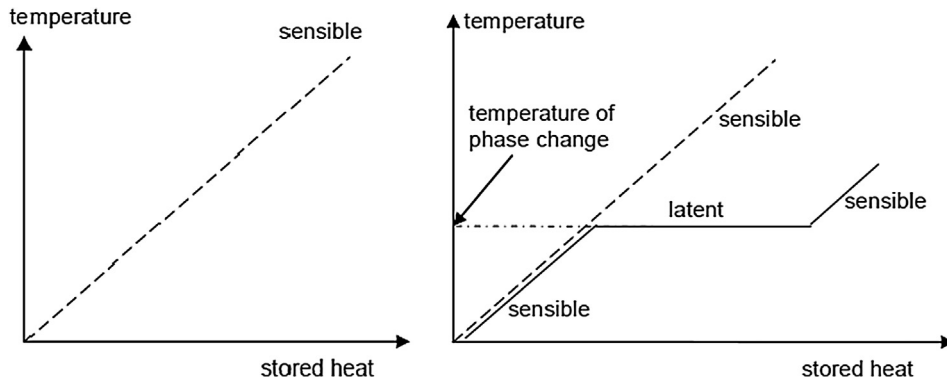


Fig. 9. Stored sensible heat (left) and stored latent heat (right) with respect of temperature (Cabeza and Mehling, 2008).

heat. Salt hydrates could also be used for solar applications. On one hand, they are relatively cheap, have sharp temperature and high thermal conductivity compared with other PCMs (Sharma and Sagara, 2013). On the other hand, they have limitations of chemical instability when they are heated, causing degradation at high temperatures (Kenisarin, 2010). Furthermore, salts in general have low heat conductivity and a relatively high degree of supercooling. A comparison of properties of organic and inorganic materials are presented in Table 3.

Lastly, compositions or mixtures of materials are presented. A eutectic composition is formed at the eutectic point (there are binary and ternary eutectic points for mixtures of two or three components) corresponding to the lowest melting point in a phase-diagram describing different mixtures. The eutectic composition thus has a single melting temperature of the containment salt whereas in non-eutectic mixtures one material is melting first, followed by the other. We have to search therefore for eutectic compositions of materials with a melting temperature suitable for our application. Their advantage is that they do not exhibit segregation (Sharma and Sagara, 2013).

In Fig. 11, a graphic of PCM with respect to heat of fusion and melting temperature is presented. For the range of temperatures studied in this review, salt hydrates and their mixtures, sugar-alcohols, paraffins and salts and their eutectic mixtures must be considered. In Fig. 12, a detailed classification of PCMs is presented.

Table 2

Properties of paraffins and non-paraffins (Khan et al., 2017).

	Advantages	Disadvantages
Paraffins	Safe Reliable Predictable Less expensive Non-corrosive Low vapor pressure	Low thermal conductivity High volume change with phase change Non-compatibility with plastic container Moderately inflammable
Non-paraffins	Thermal stability Chemical durability Non-corrosiveness Non-toxicity Easy availability Little/no subcooling Narrow temperature range	Highly inflammable Low heat of fusion Low thermal conductivity Low flash point Toxicity Instability at high temperatures

3.3. Requirements for a good Phase Change Material for thermal storage

Any latent heat TESS must contain at least these three components: a heat storage material, a container compatible with the storage material and a heat exchange surface (Abhat, 1983). If we focus on the

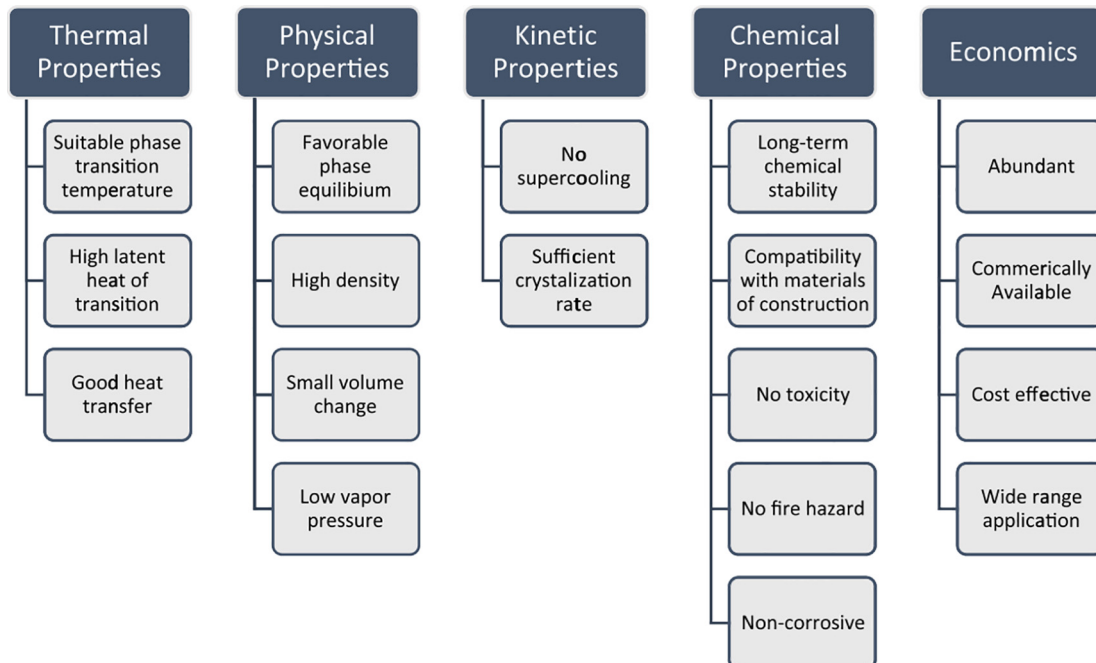


Fig. 10. Characteristics properties of latent heat storage materials (Khan et al., 2017).

**Table 3**  
Comparison of organic and inorganic materials for heat storage (Zalba et al., 2003).

Organics	Inorganics
<b>Advantages</b> No corrosives Low or none undercooling Chemical and thermal stability	<b>Advantages</b> Greater phase change enthalpy
<b>Disadvantages</b> Lower phase change enthalpy Low thermal conductivity Inflammability	<b>Disadvantages</b> Undercooling Corrosion Phase separation Phase segregation, lack of thermal stability

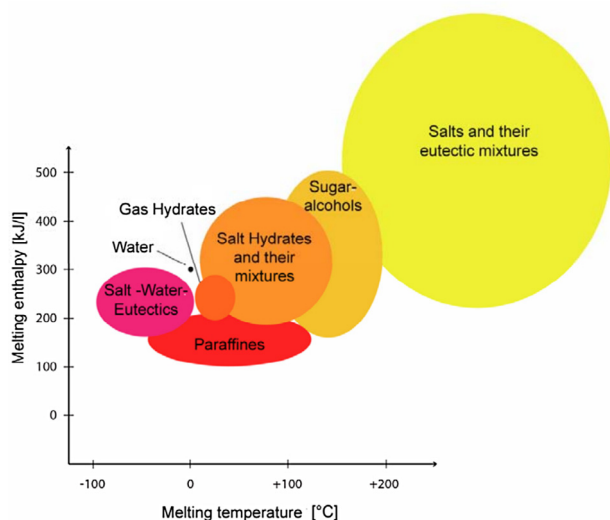


Fig. 11. PCM with respect to heat of fusion (Dieckmann, n.d.).

material, the requirements of a good Phase Change Material for thermal storage are presented below, summarizing the information previously presented by Cabeza et al. (2015), Cabeza and Mehling (2008), Gil et al. (2010) and Schroeder (1975).

### 3.3.1. Physical requirements

- Melting point that matches the range of temperatures of the application.
- High value of heat of fusion or phase change enthalpy to obtain higher storage density than sensible storage materials.
- Low heat losses.
- Reproducible phase change or cycling stability in order to use the storage material as much as longer as possible.
- No phase separation. If this effect is solved with another chemical composition the capacity of the material decreases.
- Large energy density to store the greatest amount of thermal energy per cubic meter.
- High latent heat, especially a volumetric basis to minimize the storage size.
- No subcooling or little subcooling: to avoid that during the melting and solidification process the ranges of temperature achieve wide values. The subcooling effect can be seen in Fig. 13.
- Non-toxic, non-flammable, eco-friendly.
- Good thermal conductivity so that the heat transfer during charging and discharging does not take too long time.

### 3.3.2. Technical requirements regarding the storage container

- Minimum volume variation and low vapor pressure to minimize the mechanical resistance requirements of the container and simplify the maintenance.
- Chemical and thermal stability for large number of cycles.
- Compatibility between the container and the PCM.

### 3.3.3. Economic requirements

- Low cost of the storage material in order to be able to compete with other storage technologies or even without storage (using an auxiliary gas boiler).

Kenisarin (Kenisarin and Mahkamov, 2007) pointed out that until 2007 there wasn't a good database on thermo-physical properties of PCMs and nowadays it still doesn't exist. The reasons could be the complexity of the experimental processes, the high costs and the long duration of the experiments when for example the material behavior for a high number of thermal cycles. Furthermore, there are very few publications with experimental results that allow the validation of simulation models. Some doubts exist regarding the use of PCMs in solar applications: there is not any publication that indicates which PCM is better for every solar application or a range of temperatures. Analysis for each particular case must be done.

Although a lot of PCM have been studied, none of them satisfied all the requirements of a good storage material. Hence, the storage design plays an important role to overcome the disadvantages of the material.

### 3.4. Review of potential phase change materials for medium-high temperatures

The goal of this section is to collect available latent heat storage materials for solar thermal industrial processes in a temperature range of 120–400 °C. Several publications about high temperature PCM for large solar scale applications (Gil et al., 2010; Cárdenas and León, 2013; Liu et al., 2012; Kenisarin, 2010) have been published, as well as about low-temperatures PCM for hot water, heating (Mahfuz et al., 2014; Jabbar et al., 2013; Huang et al., 2014) and cooling applications (Gil et al., 2013); (Brancato et al., 2017; Khan et al., 2017; Agyenim et al., 2015). For the present review a collection of different PCM in the studied range of temperatures has been selected from different publications.

Starting with publications of PCMs for solar cooling systems, Gil et al. (2013) presented a pilot plant to test a latent heat thermal storage system for solar cooling applications with a storage temperature range between 140 and 200 °C (Fig. 14). Although the pilot plant was not designed for process heat applications, it was included in this review because it is one of the few pilot plants tested in the studied range of temperatures considered in this study. For their experiment, they selected firstly five materials, whose characteristics can be seen in Table 4. From that list, two materials were selected to be tested in a pilot plant. They were D-mannitol and hydroquinone with melting temperatures of 162–170 °C and 168–173 °C respectively. From the experiments, the authors concluded that although D-mannitol could store more energy than hydroquinone, it showed also big subcooling during the discharging process (the subcooling effect causes that the PCM stays liquid when it should be solid because it reached the solidification temperature). Moreover, they proved that the heat transfer limitation was in the PCM and not in the heat transfer fluid (Gil et al., 2013).

In addition to the previous publication, there are several reviews about latent heat thermal storage for solar cooling applications. Mumtaz et al. (2017) presented a review of PCM, storage designs and PCM enhancement techniques for solar absorption refrigeration systems. They concluded that Erythrol, Hydroquinone and D-mannitol are

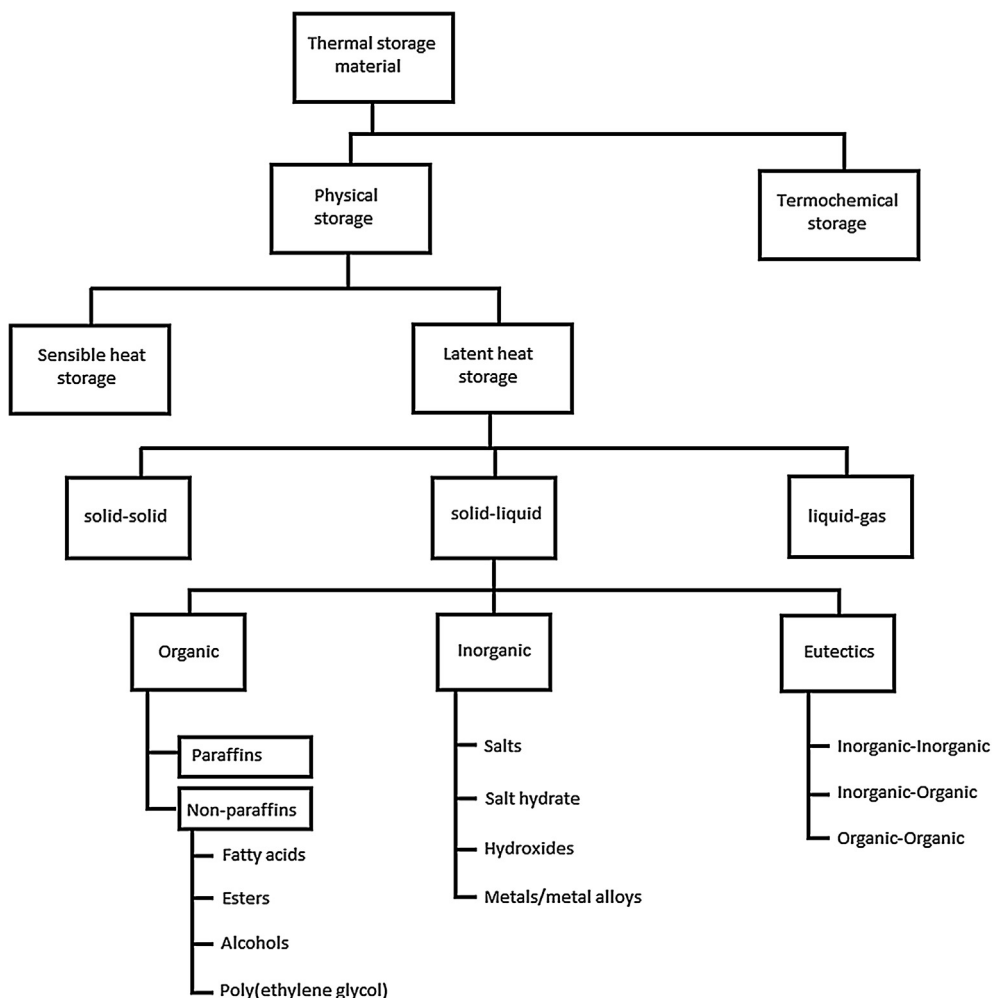


Fig. 12. Classification of PCM.

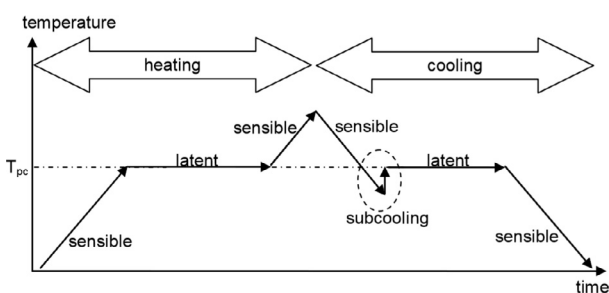


Fig. 13. Charging (heating) and discharging (cooling) with sub-cooling effect (Cabeza and Mehling, 2008).

materials often studied for the temperature range 140–200 °C. According to the authors, latent heat thermal storage (LHTS) increases the initial cost of a thermal system, but saves energy in the long-range and allows to run the system continually in spite of the discontinuity of the heat source. Pintaldi et al. (2015) presented a review of both sensible and latent heat storage materials and system designs for solar cooling applications with focused on temperatures over 100 °C where literature previously had not paid attention. The materials were separated by temperature range and by type of absorption chillers.

Besides reviews of PCM for solar cooling applications, more reviews of PCM for different range of temperatures have been published, in most of the cases for low temperature and high temperature (for CSP) applications. Sharma and Sagara (2013) presented a review of more

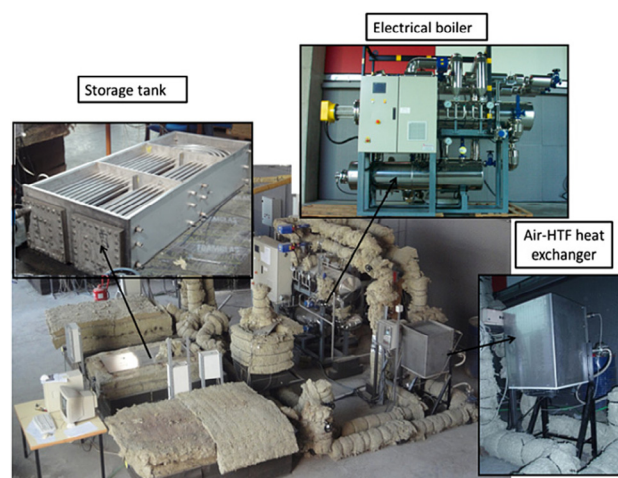


Fig. 14. Pilot plant built for solar cooling applications (Gil et al., 2013).

than 250 PCM based on previously published reviews and all commercial PCM existing until the moment. Kenisarin and Mahkamov (2007) presented three lists of some available commercial PCM of the companies EPS Ltd, TEAP Energy and Rubitherm paraffin. From the review of Kenisarin and Mahkamov (2007), just one material, the A164 (material on the basis of alkane/aliphatic solution and distributed by EPS Ltd) was suitable for the studied range of temperatures

**Table 4**  
Materials tested by Gil et al. (2013) with potential use as PCM for solar cooling.

Material	Literature phase change temperature (°C)	Experimental phase change temperature (°C)	Literature phase change enthalpy (kJ/kg)	Experimental phase change enthalpy (kJ/kg)
Salicylic acid	159	159.1(m)/111.3(s)	199	161.5(m)/109.4(s)
Benzanilide	161	163.1(m)/136.1(s)	162	138.9(m)/129.4(s)
D-mannitol	167	166.8(m)/117(s)	316	260.8(m)/214.4(s)
Hydroquinone	172.4	172.5(m)/159.5(s)	258	235.2(m)/178.7(s)
Potassium thiocyanate	173	176.6(m)/156.9(s)	280	114.4(m)/112.5(s)

m = melting; s = solidification.

**Table 5**  
Available suitable commercial PCM of the company EPL ltd.

Material	Melting temperature (°C)	Heat of fusion (kJ/kg)	Density (kg/m <sup>3</sup> )	Specific heat (kJ/kg K)	Thermal conductivity (W/m K)
A133	133	126	880	2.2	0.23
A144	144	115	880	2.2	0.23
A155	155	100	900	2.2	0.23
A164	164	290	1500	2.2	n.a
X120	120	180	1245	1.5	0.36
X130	130	260	1280	1.47	0.36
X165	165	230	1304	1.43	0.36
X180	180	280	1330	1.4	0.36
H120	120	120	2220	1.51	0.506
H160	162	105	1910	1.505	0.509
H190	191	170	2300	1.510	0.512
H220	220	100	2000	1.515	0.515
H230	227	105	1553	1.520	0.518
H250	250	280	2380	1.525	0.521
H255	254	270	238	1.530	0.524
H280	282	160	225	1.535	0.527
H285	285	85	2200	1.540	0.53
H290	292	150	1900	1.545	0.537
H300	302	130	1570	1.550	0.541
H305	305	150	2100	1.555	0.545
H320	320	70	2110	1.500	0.549
H325	327	80	2110	1.505	0.553
H335	334	80	2110	1.510	0.556
H355	353	230	2060	1.520	0.559
H380	382	225	2050	1.525	0.562
H395	395	215	2330	1.530	0.565

Comments: A: organic PCM (solid-liquid); X: solid-solid PCM; H: high temperature PCM (solid-liquid).

(120–400 °C). However, the company EPS Ltd has commercially available more PCM in addition to the A164, in the range 120–400 °C, which are shown in Table 5. Kenisarin presented another PCM review (Kenisarin, 2010), focused in this case, for high-temperature solar applications (120–1000 °C).

Zalba et al. (2003) published a review of solid-liquid phase change materials. They described potential PCM and their thermo-physical

properties already studied by researchers, as well as commercial PCM. Cárdenas and León (2013) presented a review of inorganic salt compositions and metallic alloys which are potential candidates for their use as latent storage materials at high temperatures (above 300 °C). Inorganic salts are of great interest above 300 °C, since some of these salts have a relatively high heat of fusion. But they also have some disadvantages that limit their applications, such as low thermal conductivity, high corrosion and large volume changes during melting (Liu et al., 2012). For these reasons, metallic materials appeared as another potential candidate as PCM. Metal materials and metal alloys have some disadvantages, mainly their high weight and their low stored energy rate by mass unit. On the other hand, they have several advantages, like a high latent heat of fusion per volume, high thermal conductivity, low corrosion and low subcooling. Metal and metal alloys should be considered as good candidates for latent heat storage. Metal alloys can be implemented but some considerations must be taken into account as Fernández et al. (2017) stated.

Liu et al. (2012) presented a review of potential PCM with melting temperatures above 300 °C for CSP applications. In this work, as well as for Cárdenas and León (2013) the classification is divided into inorganic salts and salt composites on one hand and into metal and metal alloys on the other hand. Most of the inorganic salts and salt eutectics considered by Liu et al. (2012) were on the bases of chlorides, nitrates and carbonates, which have low cost (Liu et al., 2012). The authors made very useful conclusions: NaNO<sub>3</sub> is the most investigated PCM, because the melting temperature is in the range of direct steam generation purpose. Regarding metal and metal alloys are feasible candidates to be used as PCM, except for their higher cost compared to the salts.

Hoshi et al. (2005) identified suitable latent heat materials to be used in CSP plants. For this purpose they presented two graphs (Fig. 15). From the graph on the left, Polyethylene, Erythritol, Mannitol, NaOH, NaNO<sub>2</sub>, NaNO<sub>3</sub>, KNO<sub>3</sub> and Sn could be considered as potential PCM. From the graph on the right, the cheapest materials are Polyethylene and Erythritol for the corresponding organic materials and alcohols.

Other authors have performed assessments of PCM to study their

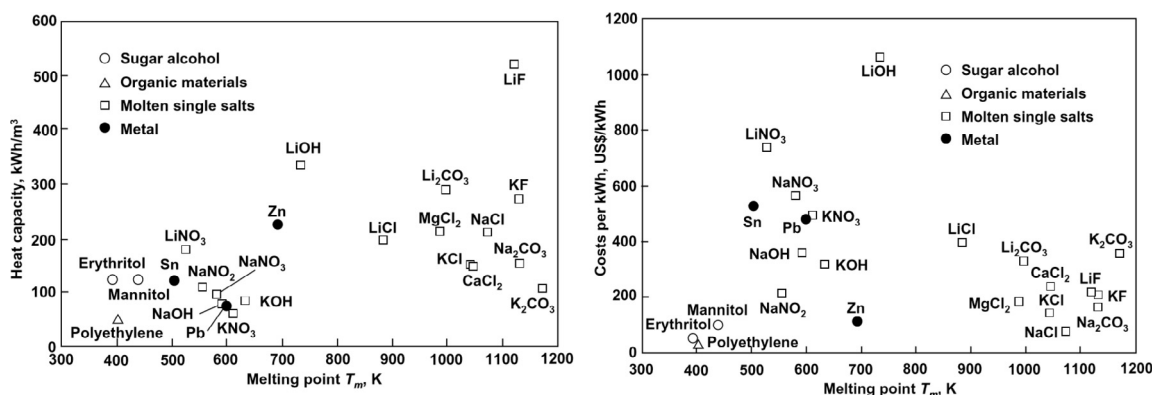


Fig. 15. Heat capacity (left) and cost per kWh (right) vs Melting point temperature (Hoshi et al., 2005).

thermo-physical characteristics. Sharma et al. (2015) presented an assessment of existing organic solid-liquid PCM and their applications for thermal storage. From their selection, almost all materials have a melting temperature below 100 °C, except for Lactitol, Maltitol, D-Mannitol, Galactitol and Myo-inositol, which have been considered in the present review. Sharma et al. (2015) concluded that organic PCM at medium temperatures (90–150 °C) are non-corrosive and exhibit reproducible melting and freezing characteristics, even after a large number of thermal cycles. Organic PCM have been tested a lot in the range 80–150 °C, but not so much for higher temperatures. Moreover, most of the studies of PCM on solar thermal application were performed in Europe, where the climate changes during the day are not so drastic compared for example with the desert, where the temperature difference between day and night can be very high.

Kakiuchi et al. (1998) made a study using erythritol, which is a sugar alcohol (organic material), as phase change material. They found out that the properties of erythritol were suitable for its use as heat storage material. For the measurements of the latent heat and specific heat of the sugar alcohols they used a DSC (Differential Scanning Calorimetry) and an adiabatic calorimeter. The results presented by Kakiuchi are shown in Table 6. Erythritol increased a 10% of its volume during solid-to-liquid phase change, therefore this must be taken into account when the container is designed. Agyenim et al. (2011) also used erythritol as PCM for a solar cooling applications.

Pincemin et al. (2008) presented a study of new composites made of salts or eutectics and graphite to analyze their enhancement properties of stability, storage capacity and thermal conductivity in a melting temperature range of 200–300 °C. Seven salts were selected for the experiments: two types of nitrates (NaNO<sub>3</sub>, KNO<sub>3</sub>), two types of hydroxides (NaOH, KOH) and three types of chlorides (ZnCl<sub>2</sub>, NaCl, KCl). Eutectic materials of these salts were also considered. Taking into account important factors, such as corrosion, hygroscopic behavior, industrial availability and cost, the NaNO<sub>3</sub>/KNO<sub>3</sub> binary system was selected. The authors concluded that the use of new composite materials made of inorganic PCM and graphite for solar applications in the range 200–300 °C could significantly enhance the performance of the storage material (Pincemin et al., 2008). However, the thermal conductivity of the composite decreased at increasing temperatures. Therefore, this material was not good enough for CSP applications. Further studies to improve thermal conductivity should be performed.

Hailot et al. (2011) presented a selection of suitable organic PCM in the temperature range of 120–150 °C based on previous publications (Khan et al., 2017; Agyenim et al., 2015; Mahfuz et al., 2014; Jabbar et al., 2013; Huang et al., 2014). The authors considered that the measurements provided in those papers were limited, therefore measurements for 11 materials were made. For the measurements, a thermogravimetric (TG) and a differential scanning calorimetry (DSC) were used to define the thermo-physical properties of the materials. The requirements for choosing the materials to be characterized were: low toxicology and ecological impact, low costs and weakly hygroscopic. The first selection of 11 materials is shown in Table 7. Once the measurements of enthalpy, stability and reliability of the phase change

**Table 6**  
Melting point, heat of fusion and cost of typical sugar alcohol (Kakiuchi et al., 1998).

Material	Melting point (°C)	Heat of fusion (kJ/kg)	Density (kg/l) (at 20 °C)	Cost (US \$/kg)
Erythritol	120	339.8	1.45	5.0
D-mannitol	166–168	316.4	1.52	6.7–7.5
Galactitol	188–189	351.8	1.47	–
Xylyol	93–94.5	263.3	1.52	6.7–8.3
D-sorbitol	96.7–97.7	185	1.50	1.1

**Table 7**  
Selection of organic PCM by Hailot et al. (2011).

Material	Phase change temperature (°C)	Heat of fusion (kJ/kg)	Density (kg/m <sup>3</sup> )	Supplier
Trometanol (TAM)	132	285	1350	Lancaster synthesis
Dimethylpropionic acid (DMPA)	185	289	–	Lancaster synthesis
Sebacic acid	130–134	228	1270	Merck
Maleic acid	131–140	235	1590	Merck
Adipic acid	151–155	260	1360	Roth
Glucose-D	149–152	174–192	–	Merck
Polyethylene (HDPE)	130	211–233	960	Aldrich
Benzoic acid	121–123	114–147	1080	Merck
Phthalic anhydride	131	159	1530	Merck
Dimethyl terephthalate	142	170	1290	Merck
Urea	133–135	170–258	1340	Roth

**Table 8**  
List of considered latent heat storage materials for Pollerberg et al. (2012).

Storage material	Temperature (°C)	Specific heat of fusion (kJ/kg)
Water (reference)	120–150	128.5 (sensible heat)
Polyethylene PE-HD	122–133	150–200
Polyethylene PE-UHM	124–134	150–200
Polyethylene Licocene PE 4201	125–130	246
Polyethylene Licocene PP 6102	142–148	70
Polyethylene Licocene PP 7502	155–165	106
KNO <sub>3</sub> -NaNO <sub>2</sub> -NaNO <sub>3</sub> (53/40/7)	142	80
Mannitol	164–167	294–325
Palatinitol (Isomalt)	145	170

process (for 4 cycles) of the 11 materials were performed, four of them were discarded. DMPA, maleic acid and urea did not show a suitable cycling stability. D-glucose showed low decomposition temperature. The results showed that only seven organic materials (TAM, sebacic acid, HDPE, adipic acid, benzoic acid, Phthalic anhydride and Dimethyl terephthalate) could be considered as potential latent storage materials for the range 120–150 °C.

Bauer et al. (2009) studied several thermo-physical and chemical stability properties of sodium nitrate (NaNO<sub>3</sub>). Its melting temperature according the author's experiments was 306 °C and its heat of fusion was 178 kJ/kg. Although there was an impact of nitrite formation during the melting phase, the authors concluded that the thermal stability of NaNO<sub>3</sub> was enough for its use as PCM.

Nomura et al. (2010) studied the thermo-chemical properties of a new PCM called NaOH/Na<sub>2</sub>CO<sub>3</sub> to be used in a heat transportation system with heat recovery purposes (Fig. 16). Its latent heat of fusion (252 kJ/kg) and its melting point temperature (285 °C) was measured and it was proved that it could be used until 350 °C. Moreover, it had little subcooling and was chemically stable for 500 h. The authors considered the PCM suitable for the application. A schematic diagram of the PCM-container is shown in Fig. 17. Shin and Kim (1990) analyzed a ternary carbonate eutectic (32.1% Li<sub>2</sub>CO<sub>3</sub>, 34.5% K<sub>2</sub>CO<sub>3</sub>, 33.4% Na<sub>2</sub>CO<sub>3</sub>) as a latent heat storage material. In the experiments, it showed a phase change transition temperature of 395–397 °C, heat transfer from 34 to 51 W/mK and no subcooling over 50 thermal cycles.

Most of the publications focus on the measure of heat of fusion and melting temperature and they leave aside other important PCM characteristics, such as charging/discharging properties, subcooling, phase segregation, thermal conductivity or behavior for a large amount of cycles. However, Rodriguez-Garcia et al. (2016) recently performed a study about the melting/freezing cycles and long-term melting stability

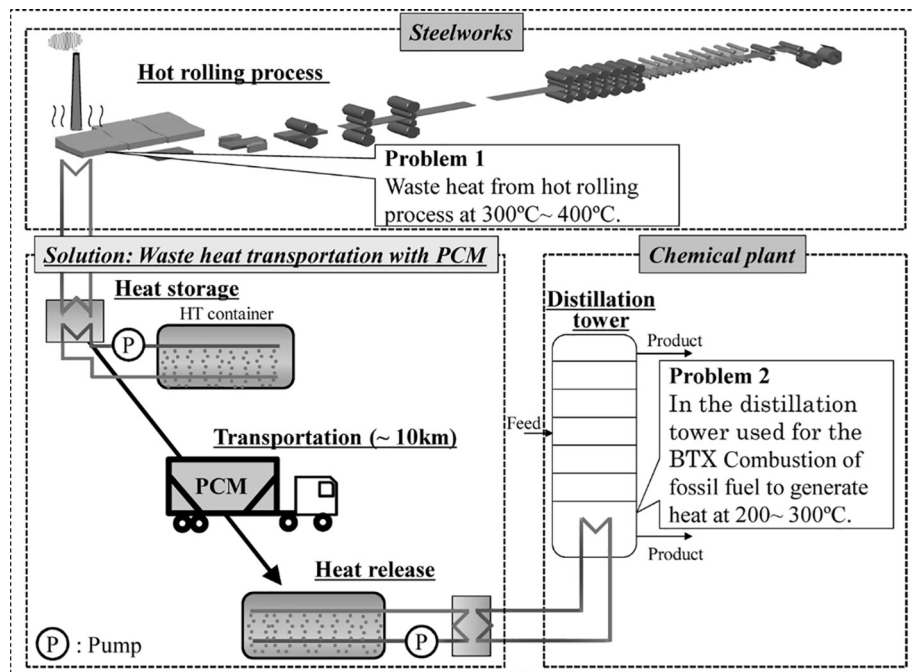


Fig. 16. Concept of the heat transportation system using PCM (Nomura et al., 2010).

tests of the D-mannitol under an inert atmosphere of Ar and N<sub>2</sub>. After testing the material between 100 and 190 °C for 50 cycles, they observed a change in the melting interval. Regarding long-term melting stability test at 180 °C a change in consistency from hard solid to soft paste and a decrease of mass was experienced. They concluded that sample degradation and production of volatile species appeared during heating. Therefore, they concluded that D-mannitol was not a feasible PCM even under inert atmosphere.

More recently, Gimenez-Gavarrell and Fereres (2017) presented a new glass encapsulated PCM for high temperature (300–400 °C) LH to be used in direct steam generation solar thermal plants. For the development of the experimental design, they used NaNO<sub>3</sub> and Pb as PCM and borosilicate as encapsulation material. The latent heat, specific heat

and melting temperatures of the two PCM considered were experimentally measured using a DSC.

Several reviews of potential PCM have been already performed (Cárdenas and León, 2013; Kenisarin, 2010; Zalba et al., 2003; Liu et al., 2012; Haillot et al., 2011). Nevertheless, no international or even national methodologies to measure the melting temperature, heat of fusion, degradation with cycles, thermal conductivity, etc. exist. Moreover, most of the times the available features of the PCM are just the melting temperature and the heat of fusion. It is obvious that a lack of proper data and standards exists. Therefore, it is difficult to provide a good and scientific recommendations about which material is more suitable for a particular application. However, in this review a collection of the most promising materials presented by different authors is

### (a) Schematic diagram of HT container

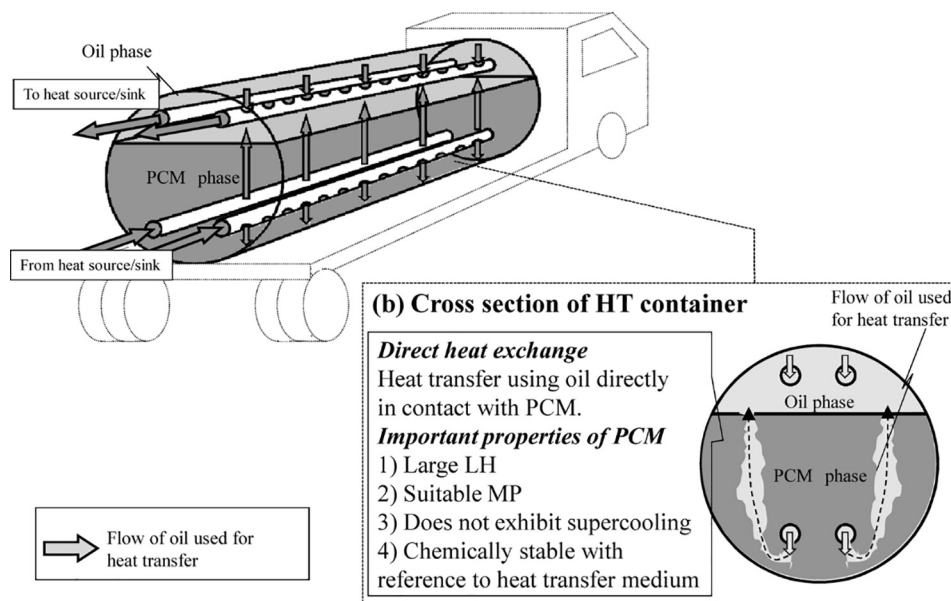


Fig. 17. Schematic diagram of the container (a) and its cross section (b) (Nomura et al., 2010).

**Table 9**  
Inorganic substances with potential used as PCMs.

Compound	Phase change temperature (°C)	Heat of fusion (kJ/kg)	Thermal conductivity (W/mK)	Density (kg/m <sup>3</sup> )	Specific heat (kJ/kgK)	Type of substance
Mg(NO <sub>3</sub> ) <sub>2</sub> ·2H <sub>2</sub> O	130 (Zalba et al., 2003)	–	–	–	–	Salt hydrates
NaC <sub>2</sub> H <sub>3</sub> O <sub>2</sub> ·3H <sub>2</sub> O	137 (Sharma and Sagara, 2013)	–	–	1450 (Sharma and Sagara, 2013)	–	Salt hydrates
NaNO <sub>3</sub>	302.6 (Gimenez-Gavarrrell and Fereres, 2017)	176.8 ± 1.9 (Gimenez-Gavarrrell and Fereres, 2017)	0.5 (Gimenez-Gavarrrell and Fereres, 2017)	2260 (Gimenez-Gavarrrell and Fereres, 2017) (solid)	1.4 (Gimenez-Gavarrrell and Fereres, 2017) (solid)	Salt hydrates
				1900 (Gimenez-Gavarrrell and Fereres, 2017) (liquid)	1.65 (Gimenez-Gavarrrell and Fereres, 2017) (liquid)	
	306 (Michels and Pitz-paal, 2007)	172 (Michels and Pitz-paal, 2007)	0.5 (Michels and Pitz-paal, 2007)	2261 (Michels and Pitz-paal, 2007) (solid)	1.1 (Michels and Pitz-paal, 2007) (solid)	
	306 (Laing et al., 2011)	175 (Laing et al., 2011)	–	–	1.5 (Laing et al., 2011) (solid)	
	306 (Bauer et al., 2009)	178 (Bauer et al., 2009)	0.514 (Bauer et al., 2009)	2260 (Bauer et al., 2009) (solid-25 °C)	1.655 (Bauer et al., 2009)	salt
				1908 (Bauer et al., 2009) (liquid-306 °C)	–	
	308 (Pilkington Solar Int. GmbH, 2000)	199.3 (Pilkington Solar Int. GmbH, 2000)	0.5 (Pilkington Solar Int. GmbH, 2000)	2257 (Pilkington Solar Int. GmbH, 2000)	–	
	310 (Muren et al., 2009)	174 (Muren et al., 2009)	–	–	–	
	310 (Steinmann and Tamme, 2008)	172 (Steinmann and Tamme, 2008)	–	2260 (Steinmann and Tamme, 2008) (solid)	0.5 (Steinmann and Tamme, 2008)	
RbNO <sub>3</sub>	312 (Cárdenas and León, 2013)	31 (Cárdenas and León, 2013)	–	1820 (Steinmann and Tamme, 2008) (liquid)	–	salt
				3685 (Cárdenas and León, 2013) (solid)	–	
				2820 (Cárdenas and León, 2013) (liquid)	–	
Pb	315.4 (Gimenez-Gavarrrell and Fereres, 2017)	20.9 ± 0.1 (Gimenez-Gavarrrell and Fereres, 2017)	29 (Gimenez-Gavarrrell and Fereres, 2017) (solid)	11,340 (Gimenez-Gavarrrell and Fereres, 2017) (solid)	0.17 (Gimenez-Gavarrrell and Fereres, 2017) (solid and liquid)	metal
				10,660 (Gimenez-Gavarrrell and Fereres, 2017) (liquid)	–	
NaOH	318 (Steinmann and Tamme, 2008)	165 (Steinmann and Tamme, 2008)	–	2100 (solid) (Steinmann and Tamme, 2008)	0.92 (solid) (Steinmann and Tamme, 2008)	salt
				2080 (liquid) (Steinmann and Tamme, 2008)	–	
KNO <sub>3</sub>	320 (Nomura et al., 2010)	159 (Nomura et al., 2010)	–	1785 (solid) (Nomura et al., 2010)	2.15 (Nomura et al., 2010)	salt
	333 (Pilkington Solar Int. GmbH, 2000)	266.1 (Pilkington Solar Int. GmbH, 2000)	0.5 (Pilkington Solar Int. GmbH, 2000)	2110 (Pilkington Solar Int. GmbH, 2000)	–	
	335 (Michels and Pitz-paal, 2007)	95 (Michels and Pitz-paal, 2007)	0.5 (Michels and Pitz-paal, 2007)	2109 (Michels and Pitz-paal, 2007)	0.953 (Michels and Pitz-paal, 2007)	
KOH	360 (Michels and Pitz-paal, 2007)	134 (Michels and Pitz-paal, 2007)	0.5 (Michels and Pitz-paal, 2007)	2040 (Michels and Pitz-paal, 2007) (solid)	1.34 (Michels and Pitz-paal, 2007) (solid)	salt
				2044 (Pilkington Solar Int. GmbH, 2000)	–	
53.7Zn/46.3Mg	340 (Akiyama et al., 1992)	185 (Akiyama et al., 1992)	–	4600 (Akiyama et al., 1992)	–	Metal alloy
52Zn/48Mg	340 (Fernández et al., 2017)	180 (Fernández et al., 2017)	–	–	–	Metal alloy
51Zn/49Mg	342/337 (Blanco-Rodríguez et al., 2014)	155 (Blanco-Rodríguez et al., 2014)	75 (Blanco-Rodríguez et al., 2014)	2850 (Blanco-Rodríguez et al., 2014)	0.73 (Blanco-Rodríguez et al., 2014)	Metal alloy
52Zn/48Mg	340 (Kenisarin, 2010), (Farkas and Birchenall, 1985)	180 (Kenisarin, 2010); (Farkas and Birchenall, 1985)	–	–	–	Metal alloy
96Zn/4Al	381 (Akiyama et al., 1992)	138 (Akiyama et al., 1992)	–	6630 (Akiyama et al., 1992)	–	Metal alloy
55Mg/28/17Zn	400 (Fernández et al., 2017)	146 (Fernández et al., 2017)	–	2260	–	Metal alloy

**Table 10**  
Organic substances with potential used as PCM.

Compound	Melting Temperature (°C)	Heat of fusion (kJ/kg)	Thermal conductivity (W/mK)	Density (kg/m <sup>3</sup> )
Erythritol	120 (Kakiuchi et al., 1998)	339.8 (Kakiuchi et al., 1998)	0.326 (liquid, 140 °C) (Kakiuchi et al., 1998) 0.733 (solid, 20 °C) (Kakiuchi et al., 1998)	1300 (liquid, 140 °C) (Kakiuchi et al., 1998) 1480 (solid, 20 °C) (Kakiuchi et al., 1998)
Polyethylene (HDPE)	100–150 (Kamimoto et al., 1985)	200 (Kamimoto et al., 1985)	–	–
Valporic acid	120 (Sharma and Sagara, 2013)	–	–	1266 (Sharma and Sagara, 2013)
Benzoic acid	121.7 (Sharma and Sagara, 2013)	167 (Sharma and Sagara, 2013)	–	1164 (Sharma and Sagara, 2013)
Stibene	124 (Sharma and Sagara, 2013)	169.4 (Sharma and Sagara, 2013)	–	1341 (Sharma and Sagara, 2013)
Benzamide	127.2 (Sharma and Sagara, 2013)	228 (Haillot et al., 2011)	–	1270 (Haillot et al., 2011)
Sebacic acid	130–134 (Haillot et al., 2011)	159 (Haillot et al., 2011)	–	1530 (Haillot et al., 2011)
Phthalic anhydride	131 (Haillot et al., 2011)	136.7 (Sharma and Sagara, 2013)	–	–
Phenacetin	137 (Sharma and Sagara, 2013)	174 (Sharma and Sagara, 2013)	–	1544 (Sharma and Sagara, 2013)
Alpha glucose	141 (Sharma and Sagara, 2013)	170 (Haillot et al., 2011)	–	1290 (Haillot et al., 2011)
Dimethyl terephthalate	142 (Haillot et al., 2011)	144 (Iwamoto and Ikai, 2000)	–	–
Trans -1,4-polybutadiene (TPB)	145 (Iwamoto and Ikai, 2000)	173 (Haillot et al., 2011)	–	–
Maltitol	145–152 (Haillot et al., 2011)	135–149 (Haillot et al., 2011)	–	–
Lactitol	146–152 (Haillot et al., 2011)	180 (Sharma and Sagara, 2013)	–	–
Acetyl - p-toluidene	151–155 (Haillot et al., 2011)	260 (Haillot et al., 2011)	–	–
Adipic acid	155 (Sharma and Sagara, 2013)	134.8 (Sharma and Sagara, 2013)	–	–
Phenyldrazone benzaldehyde	159 (Sharma and Sagara, 2013)	199 (Sharma and Sagara, 2013)	–	1443 (Sharma and Sagara, 2013)
Salicylic acid	161 (Sharma and Sagara, 2013)	162 (Sharma and Sagara, 2013)	–	–
Benzamide	166 (Barreche et al., 2013)	279 (Barreche et al., 2013)	–	–
D-Mannitol	172.4 (Sharma and Sagara, 2013)	258 (Sharma and Sagara, 2013)	–	1520 (Kakiuchi et al., 1998)
Hydroquinone	187 (Sharma and Sagara, 2013)	153 (Sharma and Sagara, 2013)	–	1358 (Sharma and Sagara, 2013)
p- Aminobenzoic	179.8 (Solé et al., 2014)	246.4 (Solé et al., 2014)	–	–
Galactitol	224–227 (Barone et al., 1990)	266 (Barone et al., 1990)	–	1470 (Kakiuchi et al., 1998)
Myo-inositol			–	–

**Table 11**  
Inorganic binary and ternary mixtures compositions with potential used as PCM.

Compound	Composition	Melting temperature (°C)	Heat of fusion (kJ/kg)	Density (kg/m <sup>3</sup> )	Specific heat (kJ/kg)
LiNO <sub>3</sub> –67KNO <sub>3</sub>	33/67	133 (Kenisarin, 1993)	170 (Kenisarin, 1993)	–	–
LiNO <sub>3</sub> –68.3KNO <sub>3</sub>	31.7/68.3	135 (Kenisarin, 2010)	136 (Kenisarin, 2010)	–	–
KNO <sub>3</sub> –NaNO <sub>2</sub> –NaNO <sub>3</sub>	53/40/7	142 (Kenisarin, 1993)	80 (Kenisarin, 1993)	–	–
LiNO <sub>3</sub> –NaNO <sub>3</sub> –KCl	55.4/4.5/40.1	160 (Kenisarin, 2010)	266 (Kenisarin, 2010)	–	–
LiNO <sub>3</sub> –KCl	58.1/41.9	166 (Kenisarin, 2010)	272 (Kenisarin, 2010)	–	–
NaOH–KOH	50/50	169–171 (Kenisarin, 2010)	202–213 (Kenisarin, 2010)	–	–
LiNO <sub>3</sub> –LiCl–NaNO <sub>3</sub>	47.9/1.4/50.7	180 (Kenisarin, 2010)	265 (Kenisarin, 2010)	–	–
LiNO <sub>3</sub> –NaNO <sub>3</sub>	57/43	193 (Kenisarin, 2010)	248 (Kenisarin, 2010)	–	–
LiNO <sub>3</sub> –NaNO <sub>3</sub>	49/51	194 (Kenisarin, 1993)	265 (Kenisarin, 1993)	–	–
LiNO <sub>3</sub> –NaNO <sub>3</sub> –Sr(NO <sub>3</sub> ) <sub>2</sub>	45/47/8	200 (Kenisarin, 2010)	199 (Kenisarin, 2010)	–	–
LiNO <sub>3</sub> –NaCl	87/13	208 (Kenisarin, 2010)	369 (Kenisarin, 2010)	–	–
LiOH–NaOH	30/70	210–216 (Kenisarin, 2010)	278–329 (Kenisarin, 2010)	–	–
KNO <sub>3</sub> –NaNO <sub>3</sub>	54/46	222 (Kenisarin, 1993)	100 (Kenisarin, 1993)	–	–
		222 (Venkatesetty and LeFrois, 1976)	117 (Venkatesetty and LeFrois, 1976)	–	–
NaOH–NaNO <sub>2</sub>	20/80	230–232 (Abe et al., 1984)	206–252 (Abe et al., 1984)	–	–
NaOH–NaNO <sub>2</sub>	73/27	237–238 (Abe et al., 1984)	249–295 (Abe et al., 1984)	–	–
NaOH–NaCl–NaNO <sub>3</sub>	78.1/3.6/18.3	242 (Abe et al., 1984)	242 (Abe et al., 1984)	–	–
NaOH–NaNO <sub>3</sub>	28/72	246–247 (Abe et al., 1984)	182–257 (Kenisarin, 2010)	–	–
NaOH–NaCl–NaNO <sub>3</sub>	55.6/4.2/40.2	247 (Abe et al., 1984)	213 (Abe et al., 1984)	–	–
NaNO <sub>3</sub> –NaOH	70/30	247 (Venkatesetty and LeFrois, 1976)	158 (Venkatesetty and LeFrois, 1976)	–	–
LiNO <sub>3</sub> –Ba(NO <sub>3</sub> ) <sub>2</sub>	97.4/2.6	253 (Venkatesetty and LeFrois, 1976)	368 (Venkatesetty and LeFrois, 1976)	–	–
LiNO <sub>3</sub> –NaCl	93.6/6.4	255 (Kenisarin, 2010)	354 (Kenisarin, 2010)	–	–
LiCl–CsCl–KCl–RbCl	28.5/43.5/13.7/13.3	256 (Kenisarin, 2010)	375–380 (Kenisarin, 2010)	–	–
NaOH–NaNO <sub>3</sub>	81.5/18.5	256–258 (Abe et al., 1984)	251–292 (Abe et al., 1984)	–	–
LiOH–LiCl	63/37	264 (Philips and Stearns, 1985)	437 (Philips and Stearns, 1985)	–	–
NaOH–NaNO <sub>3</sub>	59/41	266 (Kenisarin, 2010)	278 (Kenisarin, 2010)	–	–
		266 (Abe et al., 1984)	221 (Abe et al., 1984)	–	–
LiCl–Ca(NO <sub>3</sub> ) <sub>2</sub>	59.15/40.85	270 (Venkatesetty and LeFrois, 1976)	167 (Venkatesetty and LeFrois, 1976)	–	–
LiOH–LiCl	65.5/34.5	274 (Kenisarin, 2010)	339 (Kenisarin, 2010)	–	–
LiOH–LiCl–KCl	62/36.5/1.5	282 (Kenisarin, 2010)	300 (Kenisarin, 2010)	–	–
Na <sub>2</sub> CO <sub>3</sub> –NaOH–NaCl	6.6/87.3/6.1	282 (Abe et al., 1984)	279 (Abe et al., 1984)	–	–
NaCl–NaOH–NaCO <sub>3</sub>	7.8/85.8/6.4	282 (Philips and Stearns, 1985)	316 (Philips and Stearns, 1985)	–	–
NaOH/Na <sub>2</sub> CO <sub>3</sub>	–	285 (Nomura et al., 2010)	252 (Nomura et al., 2010)	–	–
NaNO <sub>3</sub> –NaCl–Na <sub>2</sub> SO <sub>4</sub>	86.3/8.4/5.3	287 (Venkatesetty and LeFrois, 1976)	177 (Venkatesetty and LeFrois, 1976)	–	–
NaF–NaNO <sub>3</sub> –NaCl	5/87/8	288 (Babaev, 2002)	224 (Babaev, 2002)	–	–
KOH/LiOH	60/40 a	314 (Liu et al., 2012)	341 (Liu et al., 2012)	–	–
KOH/LiOH	54/46	315 (Ruiz-Cabañas et al., 2017)	535 (Ruiz-Cabañas et al., 2017)	–	–
NaOH/NaCl/Na <sub>2</sub> CO <sub>3</sub>	77.2/16.2/6.6	318 (Abe et al., 1984)	290 (Abe et al., 1984)	–	–
LiCl/KCl/BaCl <sub>2</sub>	54.2/39.4/6.4	320 (Kenisarin, 2010)	170 (Kenisarin, 2010)	–	–
KNO <sub>3</sub> /KCl	96/4 a	320 (Liu et al., 2012)	150 (Liu et al., 2012)	–	–
KNO <sub>3</sub> /KCl	95.5/4.5	320 (Michels and Pitz-paal, 2007)	74 (Michels and Pitz-paal, 2007)	2100 (Michels and Pitz-paal, 2007)	1.21 (Michels and Pitz-paal, 2007) (solid)
LiCl/KCl/LiCO <sub>3</sub> /LiF	47.4–47.7/46.8–47/3.2–3.4/2.1–2.4	340–343 (Kenisarin, 2010)	375–380 (Kenisarin, 2010)	–	–
KNO <sub>3</sub> /KBr/KCl	80/10/10 a	342 (Liu et al., 2012)	140 (Liu et al., 2012)	–	–
LiCl/NaCl/KCl	43/33/24 a	346 (Liu et al., 2012)	281 (Liu et al., 2012)	–	–
LiCl/KCl	58/42	348 (Kenisarin, 2010)	170 (Kenisarin, 2010)	–	–
MnCl <sub>2</sub> /KCl/NaCl	45/28.7/26.3,	350 (Kenisarin, 2010)	215 (Kenisarin, 2010)	–	–
Li <sub>2</sub> MoO <sub>4</sub> /LiVO <sub>3</sub> /LiCl/Li <sub>2</sub> SO <sub>4</sub> /LiF	27.1–27.6/24.8–25.3/23.4–24.2/17.3–17.8/6.1–6.2 a	360–363 (Abe et al., 1984)	278–284 (Abe et al., 1984)	–	–
LiCl/LiVO <sub>3</sub> /LiF/Li <sub>2</sub> SO <sub>4</sub> /Li <sub>2</sub> MO <sub>4</sub>	42.0/17.4/17.4/11.6/11.6	363 (Kenisarin, 2010)	284 (Kenisarin, 2010)	–	–
NaOH/NaCl	80/20 a	370 (Liu et al., 2012)	370 (Liu et al., 2012)	–	–
MgCl <sub>2</sub> /KCl/NaCl	60/20.4/19.6 a	380 (Liu et al., 2012)	400 (Liu et al., 2012)	1800 (Liu et al., 2012)	0.96 (Liu et al., 2012) (solid)
MgCl <sub>2</sub> /NaCl/KCl	57.0–53/22.5–26.5/18.5–22.5/a	385–393 (Kenisarin, 2010)	405–410 (Kenisarin, 2010)	–	–
MgCl <sub>2</sub> /NaCl/KCl	45.4/33/21.6	385 (Kenisarin, 2010)	284 (Kenisarin, 2010)	–	–
KCl/MnCl <sub>2</sub> /NaCl	45.5/34.5/20	390 (Kenisarin, 2010)	230 (Kenisarin, 2010)	–	–
MgCl <sub>2</sub> /NaCl/KCl	50/30/20	396 (Kenisarin, 2010)	291 (Kenisarin, 2010)	–	–
MgCl <sub>2</sub> /NaCl/KCl	51/27/22	396 (Kenisarin, 2010)	290 (Kenisarin, 2010)	–	–
Li <sub>2</sub> CO <sub>3</sub> /K <sub>2</sub> CO <sub>3</sub> /Na <sub>2</sub> CO <sub>3</sub>	32.1/34.5/33.4 (Shin and Kim, 1990)	397 (Kenisarin, 2010)	276 (Kenisarin, 2010)	–	–
KCl/MnCl <sub>2</sub> /NaCl	37.7/37.3/25	400 (Kenisarin, 2010)	235 (Kenisarin, 2010)	–	–

**Table 12**  
Solid-solid PCM.

Compound	Phase change Temperature (°C)	Heat of fusion (kJ/kg)	Density (kg/m <sup>3</sup> )
Tris (Hydroxymethyl) acetic acid	124 (Sharma and Sagara, 2013)	205 (Sharma and Sagara, 2013)	–
2-Amino-2-hydroxymethyl-1, 3–propanediol	131 (Sharma and Sagara, 2013)	285 (Sharma and Sagara, 2013)	–
Trometanol (TAM)	132 (Haillet et al., 2011)	285 (Sharma and Sagara, 2013)	1350 (Haillet et al., 2011)
Cross-linked HDPE	125–146 (Sharma and Sagara, 2013)	167–201 (Sharma and Sagara, 2013)	–
2,2-Bis(Hydroxymethyl) Propionic acid	152 (Sharma and Sagara, 2013)	289 (Sharma and Sagara, 2013)	–
38.2%NPG/61.8%PE	170 (Sharma and Sagara, 2013)	147 (Sharma and Sagara, 2013)	–
Pentarythritol (PE)	185 (Sharma and Sagara, 2013)	303 (Sharma and Sagara, 2013)	–
Dimethylpropionic acid (DMPA)	185 (Haillet et al., 2011)	289 (Haillet et al., 2011)	–

shown in Tables 9–12.

Tables 9–12 present different potential PCMs in the range of temperatures 120–400 °C. Tables 9 and 10 present a list of inorganic and organic substances with potential use as PCMs. Table 11 presents a list of inorganic eutectics compositions with potential use as PCMs. To end, Table 12 shows a list of solid-solid PCMs with potential use as PCMs. The PCMs from Tables 9–11 are materials with a solid-liquid phase change.

### 3.5. PCM candidates for industrial solar heat applications

In previous sections, a review of all potential PCM available in literature was presented. In this section, we want to highlight promising materials for industrial solar heat applications, especially considering the considered temperature range.

Erythritol, Hydroquinone and D-mannitol, all of them organic substances, tested to be the most promising PCMs for temperatures below 180 °C due to their high heat storage capacity. Some authors highlighted D-mannitol as a good PCM for heat storage applications. However, further experiments on D-mannitol should be performed since, in a recent publication Rodríguez-García (Rodríguez-García et al., 2016) discarded it due to degradation and production of volatile species during heating and due to this material presents polymorphism transformation which is difficult to control (Gil et al., 2013). In general, organic substances are very suitable PCMs for temperatures below 180 °C.

For temperatures above 300 °C, inorganic substances are the type of substances mainly investigated and described in the publications. NaNO<sub>3</sub>, is a promising inorganic substance for applications of industrial processes with demanding temperatures around 305 °C, especially in direct steam generation applications in CSP plants because its phase change temperature is suitable for the conditions of Rankine cycles. NaNO<sub>3</sub> has been tested for CSP applications as sensible heat storage and it doesn't have technological impediments from a system point of view for its implementation. Furthermore, by using its heat of fusion, its storage capacity is increased in comparison with its use as sensible heat. In addition, NaNO<sub>3</sub> has been used by different authors considering it as a good candidate for latent heat thermal storage systems.

Inorganic binary or ternary compositions are the largest group for potential materials, with a wide range of temperatures, from 133 to 400 °C and with the highest heat of fusion. Therefore, inorganic compositions such as the widely used commercial Solar Salt (60% NaNO<sub>3</sub>:40% KNO<sub>3</sub>) would be interesting. However, we have to look for the eutectic mixtures in order to have the same freezing and melting temperature. Further experiments are necessary to prove their properties in practice, to investigate material compatibility with steel or other construction materials, and to investigate subcooling or other unwanted properties. Also a selection for specific temperature requirements has to be made, and cost considerations have to play a role in the selection.

Not enough experiments have been performed on solid-solid PCMs, and therefore it is not possible to make a reliable selection based on the available information.

## 4. Latent heat storage systems at medium-high temperatures

### 4.1. PCM integration in experimental systems

Some latent thermal heat storage design concepts have been tested in pilot plants to assess their performance for their integration in hot water or steam generation processes. Pollerberg et al. (2012) presented a plant concept of a steam jet ejector chiller (SJEC) with latent heat and cold storage integration for a solar cooling plant. The solar field consisted on evacuated tube collectors. The authors considered several PCM for the hot storage (Table 8). After performing preliminary tests, polyethylene was finally selected because of its high specific heat of fusion and its good thermal stability. The heat storage design consisted of five latent heat storage modules with 120 MJ of latent heat and a vessel with 30 MJ sensible heat (Fig. 18), with a maximum design temperature of 145 °C. This design was able to produce 62.5 kg of steam or run the SJEC for at least 15 min at full load. Joemann et al. (2016) presented a pilot plant which consisted on a system (based on the already proposed system of Pollerberg et al. (2012)) for solar thermal process steam and chilled water generation with integrated latent heat and cold storage. The water steam was directly generated in the solar field (DSG) formed by evacuated tube collectors at around 150 °C. The selected latent heat storage material was polyethylene PE-8110 with a melting point of 130 °C. The latent heat storage worked in parallel to the steam drum. The PCM was integrated in an aluminum lamella heat exchanger. A technical drawing of the steam generation unit and the pilot plant are shown in Fig. 19.

Bhale et al. (2015) presented an experimental analysis of a concentrating solar system with sensible storage and with combined sensible and latent heat storage systems. A heat exchanger was designed for the specific purpose of containing the PCM. The latent heat storage material used was stearic acid. After the tests, the authors concluded that the system with a combined storage system has higher overall than the system with just sensible storage. Images of the experimental set-up are shown in Fig. 20.

A pilot scale latent heat thermal energy storage plant was experimentally and numerical studied by Garcia et al. (2015). The experimental storage pilot plant was integrated to the LHASA test facility in France for testing its behavior under similar conditions of commercial DSG CSP plants. The PCM storage unit consisted on a heat exchanger composed of tubes for the water-steam and an envelope housing the PCM. The PCM selected was pure NaNO<sub>3</sub>. The authors concluded that the storage system had high energy quality during discharge and very good repeatability. Fig. 21 shows a scheme of the test facilities and the real PCM storage unit.

Another latent heat thermal storage prototype was developed and tested by Bayón et al. (2010) at the Plataforma Solar de Almería (PSA) for direct steam generation purpose for CSP plants. Water steam generated by parabolic-through collectors exchanges heat with the selected PCM, KNO<sub>3</sub>/NaNO<sub>3</sub>. The storage unit consists of a tube embedded in the PCM block which contains fins in a sandwich configuration (Fig. 22). After the testing, it was observed that the stored/delivered energy provided by the storage unit was lower than expected.

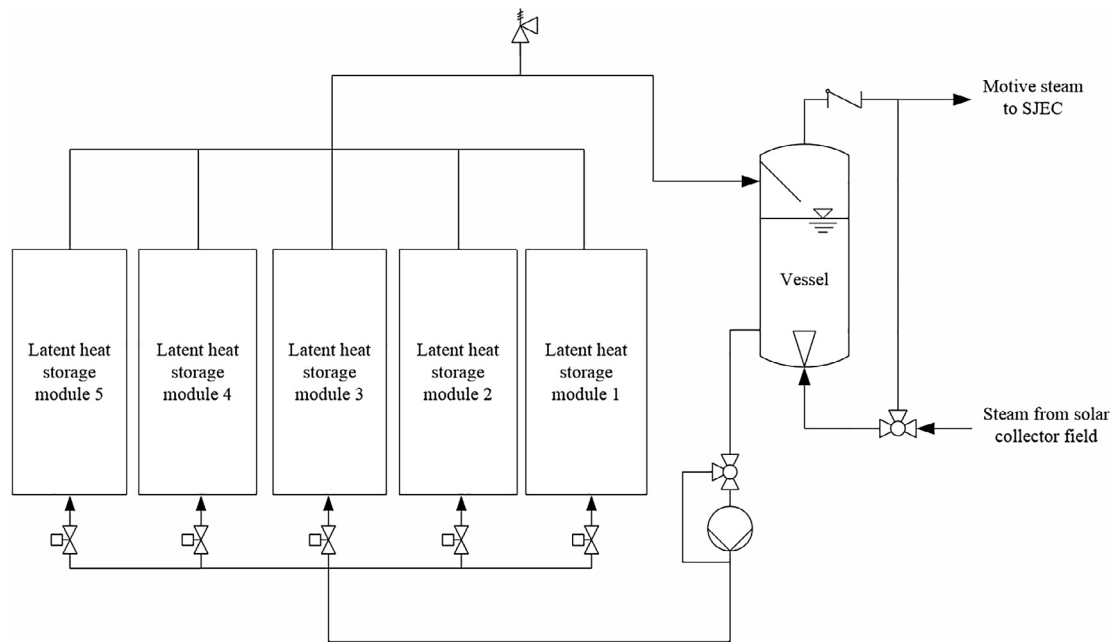


Fig. 18. Scheme of the heat storage unit with PCM (Pollerberg et al., 2012).

According to the authors, the reasons could be an insufficient amount of insulation and an excess of the amount of PCM, which didn't allow the identification of the end of the charging process. Also in the PSA, another latent heat thermal storage pilot plant was built and tested to assess its possible integration in a mini CSP Plant in Tunisia (Willwerth et al., 2017). For the testing of the latent heat storage unit saturated steam at different temperatures up to 170 °C was delivered by a steam boiler for charging and hot water up to 130 °C was provided for discharging. The tested PCM material was Hitec salt, commercially sold and usually used as molten salt utilizing its sensible heat. In this case the intention was to assess its latent heat storage performance. This salt has a melting point of 142 °C. During the charging and discharging processes (Fig. 23) solid to solid transitions (90 °C-charging; 60 °C-discharging) caused by subcooling were observed. In addition the stored latent heat was lower than expected. Because of these reasons together with the low heat of fusion of Hitec salt Willwerth et al. (2017) concluded that it is not a suitable material to be used as latent heat storage. A picture of the PCM test facility is shown in Fig. 23.

A test facility of a medium temperature concentrating solar collector integrated with thermal energy storage for industrial heating was presented by Li et al. (2017). The integrated systems were formed by solar receivers with built-in shell and tube latent PCM. In Fig. 24 a sketch of the cylindrical tank is shown. Selected PCM was the eutectic mixture of

$\text{KNO}_3\text{-NaNO}_2\text{-NaNO}_3$  with a melting temperature of 142 °C. Although the collectors performance was evaluated experimentally, its performance with the LHTES was studied numerically. The results showed that the integration of the storage for industrial heating system would increase the costs by ~10%, however it could raise the annual thermal energy gained by up to ~20%.

In addition to the pilot plants, new innovative heat exchangers designs with the integration of PCM have been presented and tested. Zipf et al. (2013) developed a prototype of a new design concept of a screw heat exchanger (SHE) with PCM integrated. The SHE allows the transportation of the latent heat storage material during the phase change. The PCM selected was a eutectic mixture of  $\text{NaNO}_3$  and  $\text{KNO}_3$  with a melting point of 221 °C. The SHE (Fig. 25) was designed for its application on large scale solar thermal power plants. The charging process of the SHE is shown in Fig. 25. Johnson et al. (2014) presented another concept design of a flat plate heat exchanger with the integration of latent heat storage material. This design substitutes the second heat exchanger fluid with isolated chambers of PCM. The heat was transferred across the steel encasements to the storage medium thanks to the primary heat transfer fluid, which flows through one side of the flat plate thermal storage. The selected material is  $\text{NaNO}_3\text{-KNO}_3$  (46–54%).

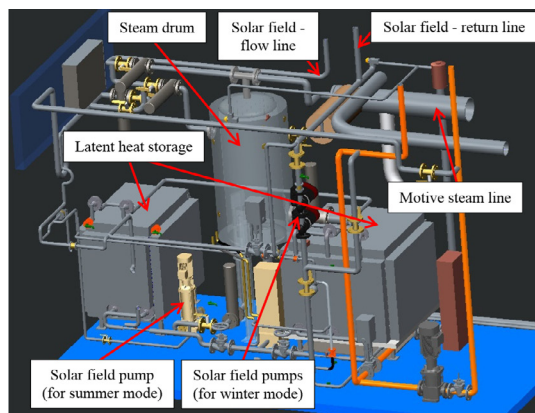


Fig. 19. Technical drawing of the steam generation unit (left) and pilot plant (right) (Joemann et al., 2016).



Fig. 20. Experimental set-up of the system presented by Bhale et al. (2015).

#### 4.2. Modelling of medium-high temperature storage systems

In literature several models to simulate PCM phase change process, LHS systems performance, charging/discharging processes and different system configurations been performed recently. The most common type of configuration modelled is the shell and tube configuration, follow by the packed bed configurations.

##### 4.2.1. Cylinder-tubes geometry

Several authors have developed simulations of PCM in shell and tube configurations. Fan et al. (2014) presented a numerical modelling of a latent heat thermal storage combined with a double-effect H<sub>2</sub>O absorption cooling system powered by solar thermal energy. The numerical model considered a simplification of the shell and tube LHTS

system, in which was considered just two concentric tubes of PCM and HTF (Fig. 26). PCM considered for this study was hydroquinone. The model of the PCM was based on the enthalpy method and some assumptions were considered: PCM was homogeneous and isotropic; radial heat transfer as well as natural convection of the PCM in the liquid phase were neglected. The mathematical model was validated with data from other publication (Trp, 2005). The authors highlighted that for this configuration natural convection cannot be neglected in the solidification process. Niyas et al. (2017) developed a 3D mathematical model for the performance investigation of a latent heat storage prototype with shell and tube exchanger configuration. For the simulation of the latent heat, the effective heat capacity method was used and for the consideration of the buoyancy effect of the molten layer in the PCM the Boussinesq approximation was considered. In addition, was

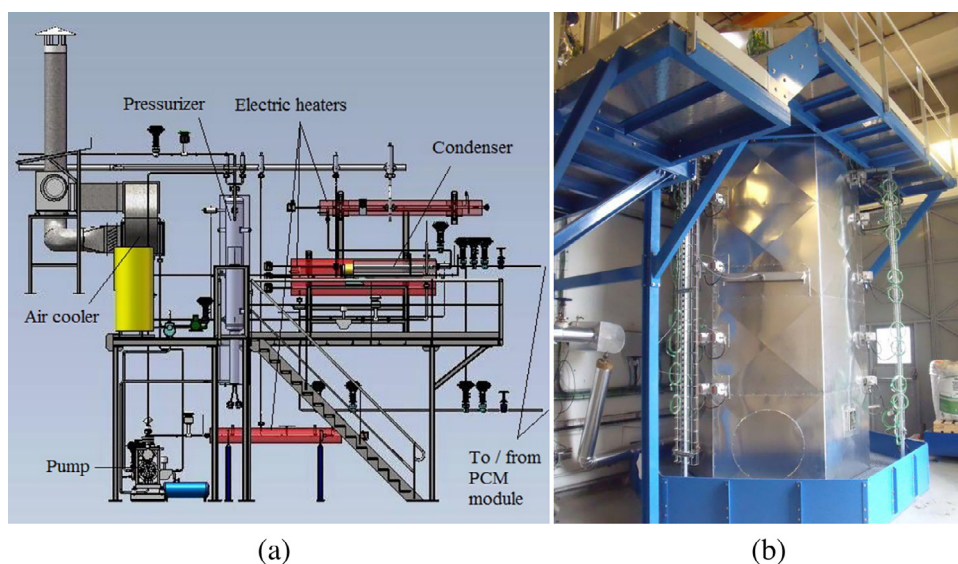


Fig. 21. Scheme of LHASA test facility (a), PCM storage unit (b) (Garcia et al., 2015).

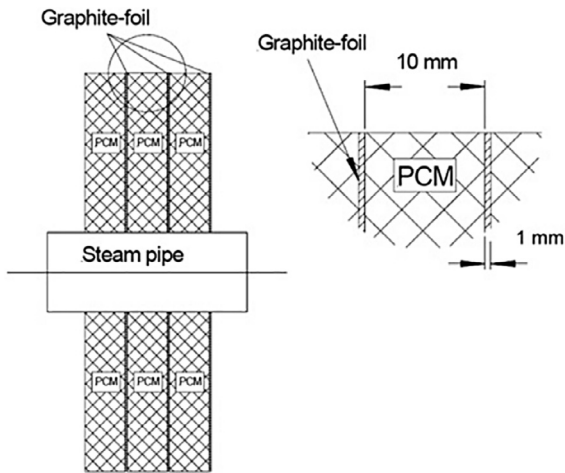


Fig. 22. Scheme of PCM/fins sandwich configuration (Bayón et al., 2010).

assumed that the phase change occurs in a temperature interval and that the PCM is homogeneous and isotropic. The equations of the model were calculated using CFD with the software COMSOL Multiphysics 4.3a. The selected PCM had a melting point of 142 °C. The temperature profile of the model during charging and discharging in comparison with experimental results presented good coincidence.

Fornarelli et al. (2017) presented a numerical simulation of the stabilization-charging and discharging processes of a vertical shell and tube latent thermal energy storage system. The selected PCM was a molten salt with melting temperature of 225 °C. 2D-axisymmetric model of the LHTS system (Fig. 26) was performed using traditional Navier-Stoke equations for the simulation of the HTF and a corrected Navier-Stoke equations for the simulation of the phase change of PCM. For the modelling of the buoyancy effect on the liquid phase the Boussinesq approximation was used. In addition, external dissipation through the walls are considered. The numerical model results were compared with experimental tests performed by the authors resulting in a good agreement between them. Besides Fornarelli, other authors focused on studying the charging/discharging cycles of PCM. Hoshi et al. (2005) developed a model for the numerical analysis of the charging and discharging performance of PCM, two of them in particular  $\text{KNO}_3$  and Pb. For this analysis the authors followed some assumptions: constant physical properties of the PCM, constant volume during phase change and natural convection in the liquid region was neglected. For the resolution of the equations the Successive Over-Relaxation (SOR)

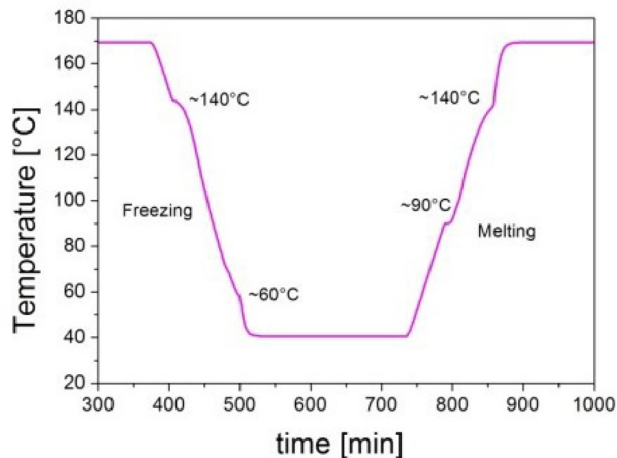
method was used. A drawing of the considered model is shown in Fig. 27. The model was thought for Concentrated Linear Fresnel Reflectors (CLFR) applications. A solar DSG plant and a CLFR Power Plant with latent heat thermal storage can be seen in Fig. 29.

In addition to simulations of latent heat thermal shell and tube heat exchangers, other simulations which consider cylindrical geometry have been published. Garcia et al. (2015) presented a pilot latent heat thermal energy storage plant located on the LHASSA facility in France, which was already mentioned. In addition to the pilot plant, a dynamic model of the latent heat thermal storage for system performances evaluation within the Dymola platform was performed. The model was based on a strictly conductive object-oriented approach in which equivalent thermal resistance was integrated. The equivalent thermal resistance was calculated by CFD. The model was validated with the tests performed in the storage test unit.

Morisson et al. (2008) presented a numerical simulation of a latent heat storage unit which took into account the solid/liquid and water/vapour phase change processes occurring simultaneously in the PCM and in the heat transfer medium. Mathematical models were developed following some assumptions: uniform and independent radial fluid flow velocity in the heat exchanger as well as axial heat conduction in the fluid was neglected; heat transfer within PCM is controlled by conduction. They developed a second and simplified model which assumed that axial thermal conduction could be neglected in both the fluid and the PCM. The storage design was considered as a fluid-tube PCM, as can be seen in Fig. 28. This model was developed for DSG applications. An example of the charging and discharging process of TESS in a DSG system can be also seen in Fig. 28.

Guo and Zhang (2008) presented a numerical simulation to assess the heat transfer enhancement of a PCM with aluminum foils during the discharging process. Fluent 6.2. was used for the simulation. A parametric analysis of the influence of the geometry, thermal and boundary conditions was also carried out. The selected material for the analysis was  $\text{KNO}_3$ - $\text{NaNO}_3$ , commonly selected for DSG applications. The storage design consisted in a foil-tube arrangement as can be seen in Fig. 30. The enthalpy-porosity method was used to perform the model. Constant thermophysical characteristics of the PCM were considered in the simulation, as well as pure conduction for the solid phase.

Bayón et al. (2010) studied the applicability of a latent heat storage model compounded of PCM-graphite sandwich arrangement using the quasi-static approximation. For this approach they assumed that during charging/discharging the storage material remains at its melting temperature. Comparing the simulated and the measured results the authors concluded that generated vapor was unequal along the pipe and



(a)



(b)

Fig. 23. Hitec freezing-melting (charging-discharging) curve (a) and PCM test facility (b) (Willwerth et al., 2017).

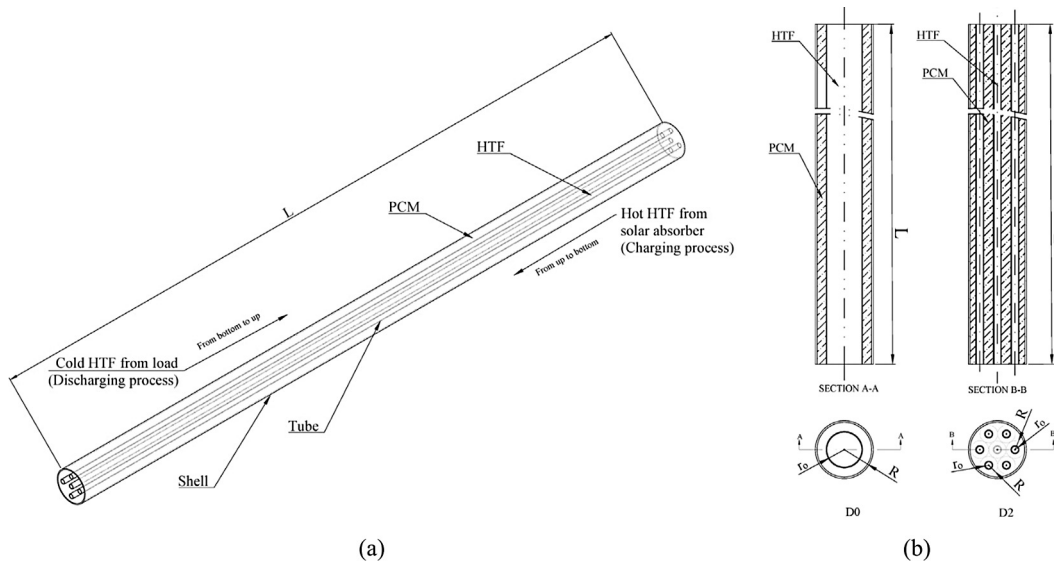


Fig. 24. View of the cylindrical tank (a); cross-section view of the cylindrical tank with 1 tube and with 7 tubes in the shell (b) (Li et al., 2017).

also its behavior depended on its position. Moreover, they reported that the quasi-static approach cannot be applied at the beginning of charging and end of the discharging because the sensible heat is not negligible on that stage.

The software Modelica have been used recently to model PCM in different configurations. Buschle et al. (2006) used Modelica to model a steam accumulator with the addition of PCM as an external element to study the performance of the system (Fig. 31). Several PCM materials in the adequate range of temperatures of the present study are suitable for the modeling such as,  $KNO_3$ ,  $NaNO_3$  or Pentaerythritol. The thermal behavior of a cylinder of PCM was simulated via discretization of the PCM into radial layers. Three ways to calculate the enthalpy of the PCM storage system were compared. The first method was a linear interpolation using If-, Elseif- and Else-clauses, the second method is based on an arc tangent function and for the third method the error function was used. These methods were performed in the Modelica.Media package.

Michels and Pitz-paal (2007) tested experimentally a cascaded latent heat storage (CLHS) system (Fig. 32) with three alkali nitrate salts within a range of melting temperatures between 306 and 335 °C. In addition, they developed a model of a CLHS system, which was validated with the experimental results. For the simulation of the CLHS some assumptions were considered: the PCM was considered as a

lumped mass with a uniform temperature throughout and the overall heat transfer coefficient was considered independent of time and axial position along the CLHS. To obtain a numerically stable model only radial discretization was used. In the liquid phase natural convection for heat transfer was considered and in solid phase transient heat conduction was considered. The software Dymola/Modelica was used to perform the simulation.

Stückle (2009) presented the modelling of a modular sensible-latent heat storage system (Fig. 33) for Direct Steam Generation (DSG) using also the software Modelica. Since the saturated temperature range of saturated steam is between 200 and 320 °C, nitrate salts were used as PCM. The modular heat storage system consisted of a sensible heat preheater and superheater and a latent heat evaporator. To model the PCM storage a cylindrical storage element was discretized in axial and radial directions. The discrete elements are shown in Fig. 33. In the model was assumed that PCM was treated as a solid for both liquid and solid phases.

4.2.2. Packed bed

In the last years, some authors have focused on the modelling of packed bed latent heat thermal storage systems and on its integration with solar thermal applications. Yagi and Akiyama (1995) developed a simulation model of a single PCM spherical capsule and of the heat

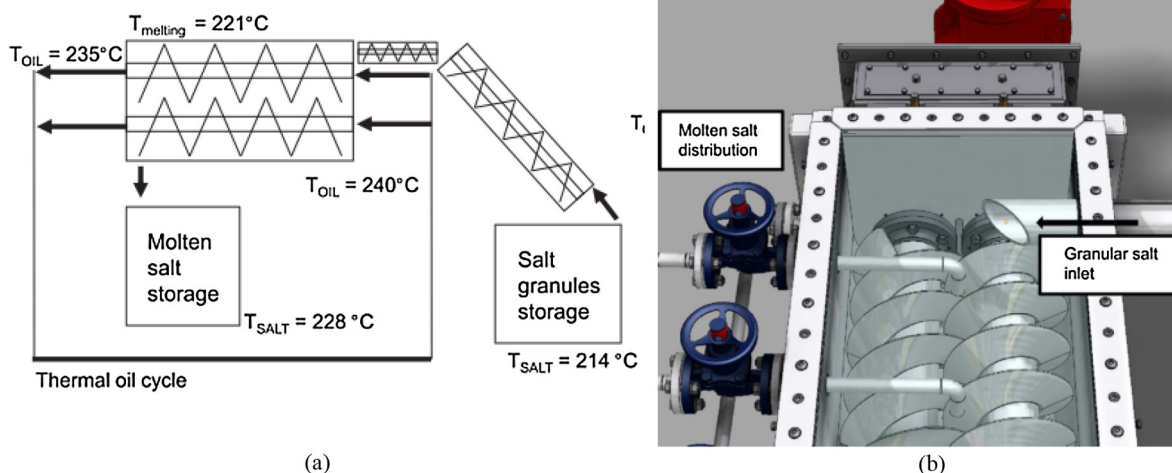


Fig. 25. Storage system during charging (a) and inside of the SHE (b) (Zipf et al., 2013).

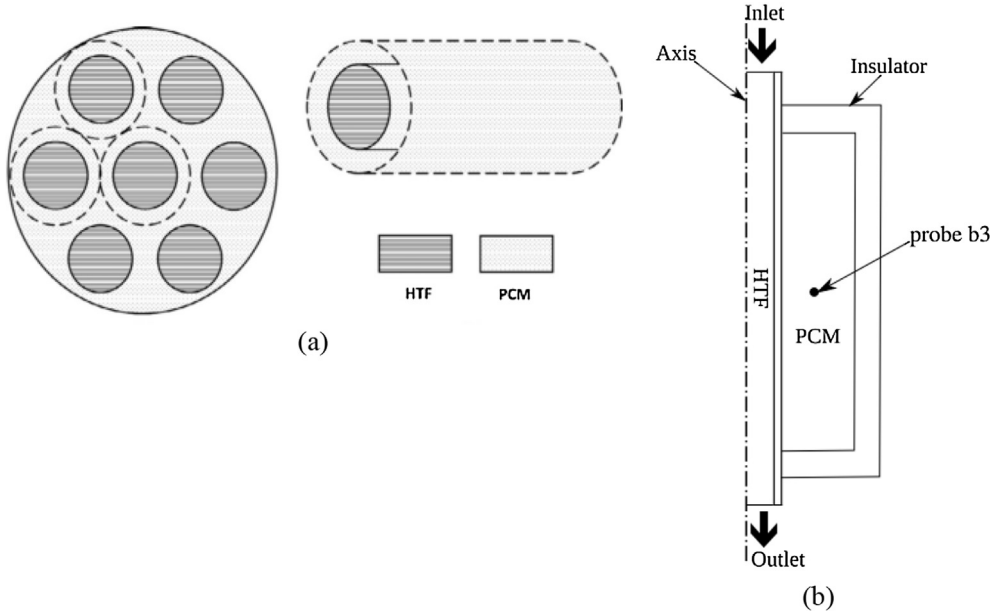


Fig. 26. Shell-and-tube LHTS configuration (left) and simplified model (right) (a) (Fan et al., 2014); Sketch of the vertical shell and tube heat exchanger (b) (Fornarelli et al., 2017).

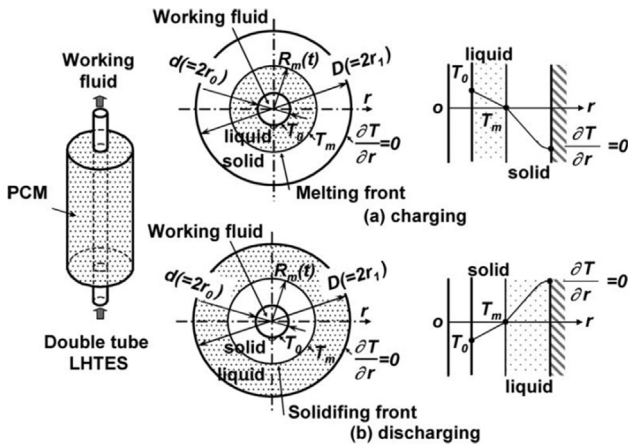


Fig. 27. Model considered for the simulation of LHTES by Hoshi et al. (2005).

transfer in a packed bed filled with spherical PCM capsules for temperatures above 500 °K. The enthalpy method was used for the heat transfer simulation assuming that both convective and radioactive heat transfer occurs and that the PCM volume during phase change stays constant. For the discretization of the gas flow across the packed bed the control volume method was used and for its calculation the SIMPLE method. Shamsi et al. (2017) presented a performance evaluation and optimization of a encapsulated cascade latent thermal storage system. To solve the dimensionless equations the method of characteristics was used; for the optimization of the CLHS system genetic algorithm was applied. The authors assumed for the development of the model constant properties of PCM and disregarded the conduction heat transfer in vertical direction. For the optimization of the CLHS different PCM were considered:  $KNO_3$ ,  $NaNO_3$ ,  $NaOH$ ,  $KOH$  and  $ZnCl_2$ , as well as different lengths of cascade stages. The model was validated with experimental work (Nallusamy et al., 2007). An sketch of the CLHS system is shown in Fig. 34.

The used of packed bed configuration combined with PCM and solar

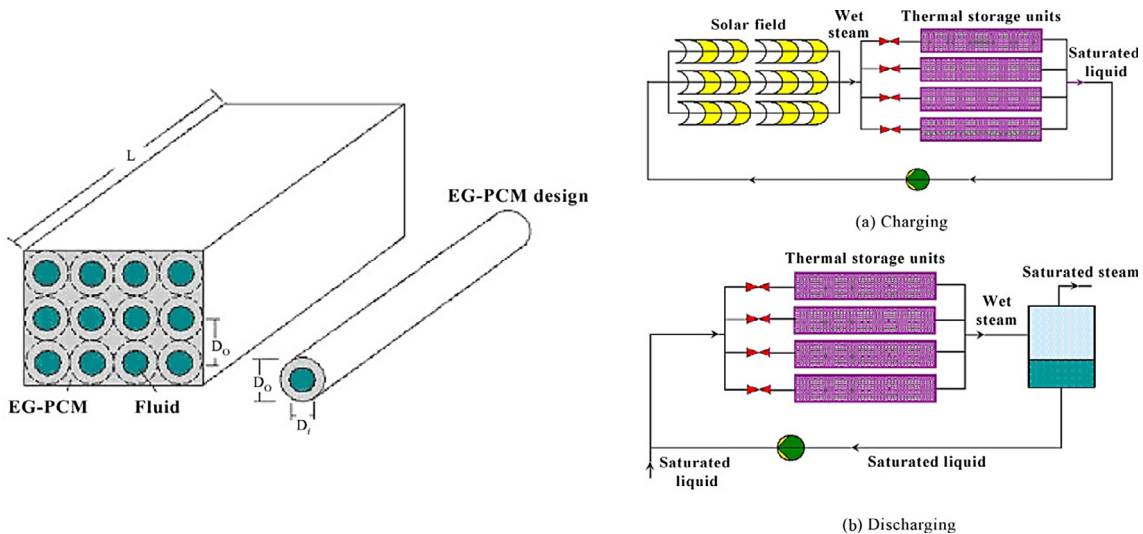


Fig. 28. Configuration of a single storage block (left); Control schemes during charging and discharging mode of a DSG Plant with TES (right) (Morisson et al., 2008).

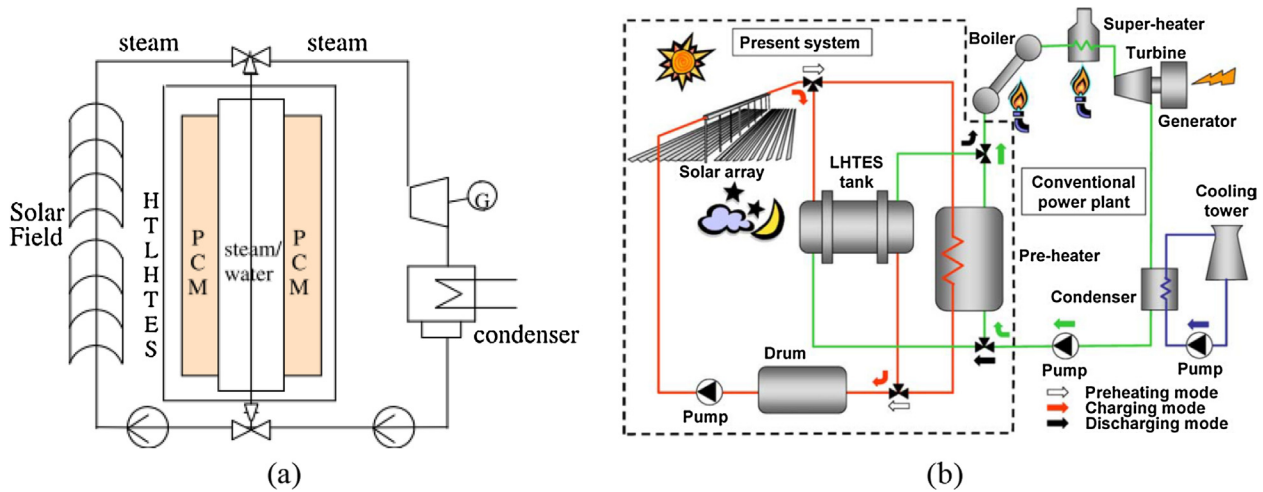


Fig. 29. Application possibilities of PCM storage systems: DSG plant (a) (Guo and Zhang, 2008) and CSP Power Plant (Hoshi et al., 2005) (b).

thermal applications have been considered by some authors. Manfrida et al. (2016) developed a mathematical model of a latent heat storage (LHS) system within EES environment and simulated its integration under dynamic conditions into an solar-powered Organic Rankine Cycle. The LHS system consisted of a cylindrical vessel filled with encapsulated PCM spheres of Paraffin. To perform the mathematical model the following assumptions were considered: the storage vessel was divided in  $N_x$  control volumes from the bottom to the top; radial conduction was neglected, as well as the axial conduction in the HTF. The model of the LHS was validated with experimental data from publications. Sections of the storage vessel are shown in Fig. 35 ( $T_P$ : temperature of PCM,  $T_F$ : Temperature of HTF and  $T_{ST}$ : temperature of the wall). The simulation of the whole system was performed in TRNSYS. The results of the system performance simulation showed that it could provide power in 78,5% of the time.

Bhagat and Saha (2016) presented a numerical analysis of a packed bed of spherical encapsulated latent heat thermal energy storage system to study its behavior facing fluctuations during charging and discharging cycles coupled with a solar-powered ORC. The model considered the enthalpy method to simulate the phase change of the PCM and two-temperature non-equilibrium energy equation for the heat transfer. The

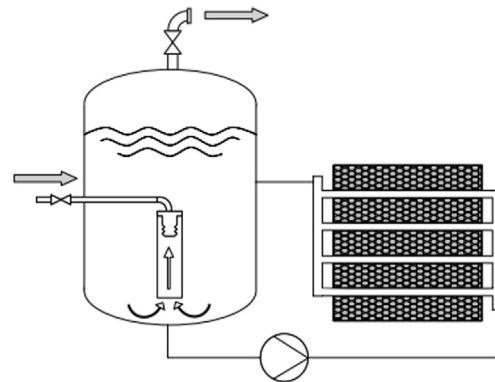


Fig. 31. Steam accumulator with PCM (Buschle et al., 2006).

authors assumed for the model: constant thermophysical properties of PCM and HTF; isothermal phase change and constant volume of the PCM. The 2D axisymmetric domain is shown in Fig. 36. The selected material was the commercial material A164, sold by EPL Ltd.

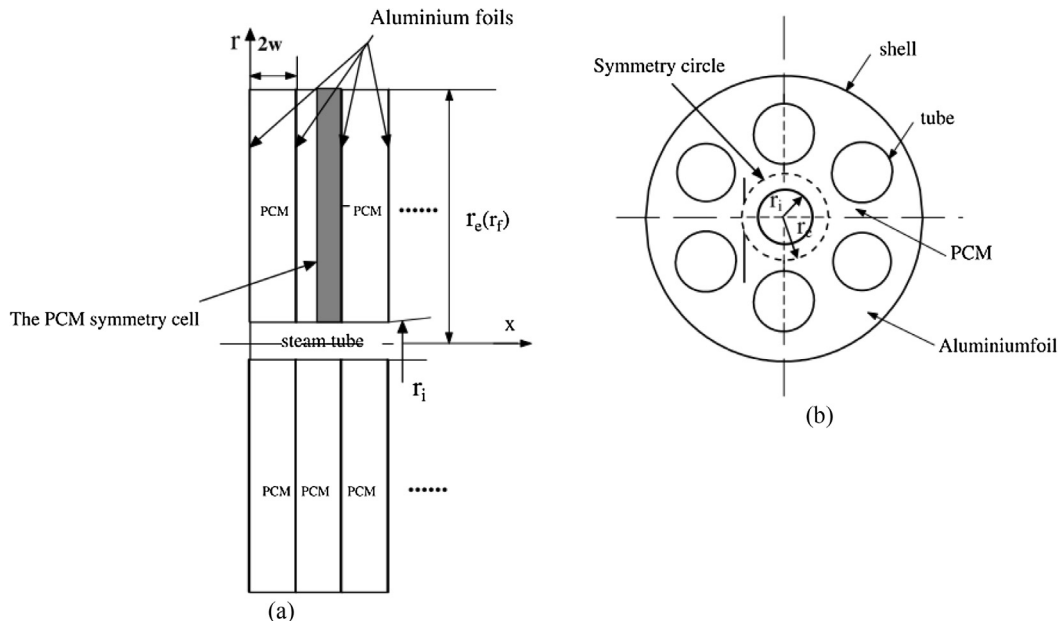


Fig. 30. Design of the PCM system, axial view (a) and transversal view (b) (Guo and Zhang, 2008).

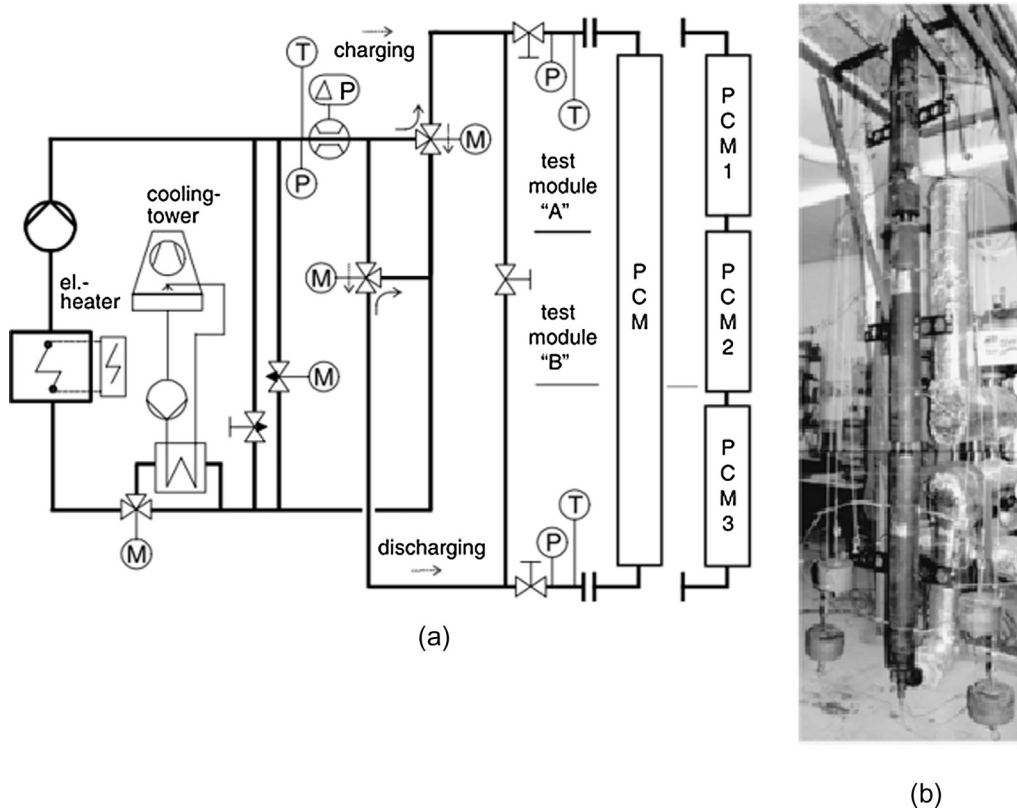


Fig. 32. Flow diagram of the thermal oil test facility (a). Test module B (b) (Michels and Pitz-paal, 2007).

Parametric studies of different parameters were also performed. The numerical model was validated with experimental work (Nallusamy and Velraj, 2009). Another numerical analysis for the optimization of a packed bed thermal energy storage system coupled with solar thermal heat source was developed by Bellan et al. (2014) for CSP applications. The packed bed was filled by spherical capsules of sodium nitrate. The enthalpy method was applied for the simulation of the phase change process and the Brinkmann equation was used to model the axial

velocity along the radial direction of the HTF through the tank. Conductivity on both solid and liquid phase was considered. To solve the equations the authors assumed: an axisymmetric system, the PCM capsules behave as a continuous medium and radiation heat transfer between the spheres was neglected. The model was validated using previous models of the authors.

Galione et al. (2014) presented a numerical simulation of a new multi-layered solid-PCM (MLSPCM) thermozone thermal storage

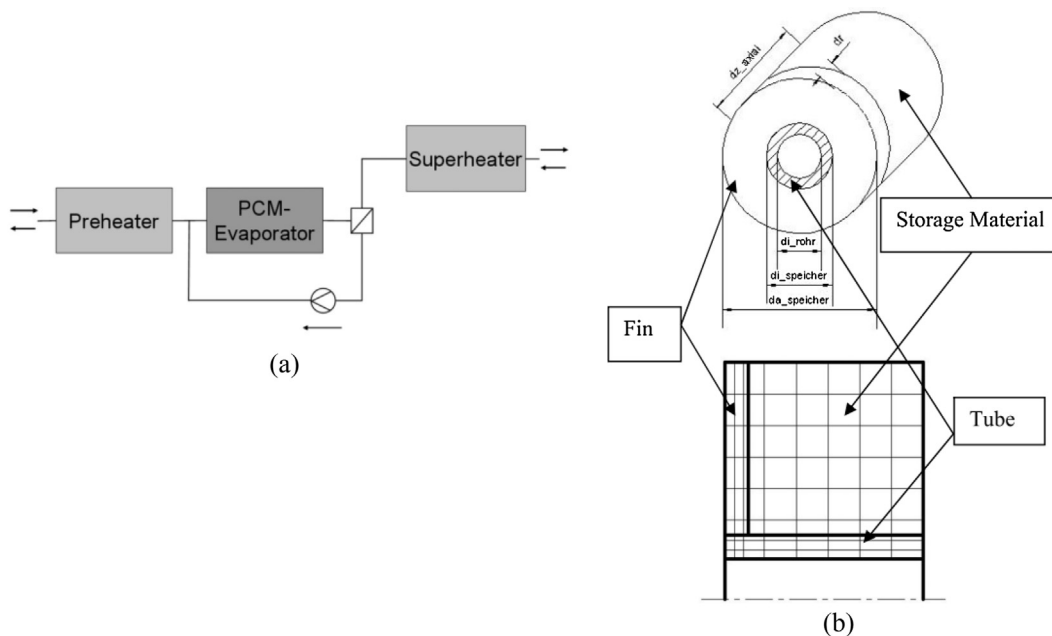


Fig. 33. Modular storage system (sensible storage-PCM) (a); Model and two-dimensional grid of storage tube (b) (Stückle, 2009).

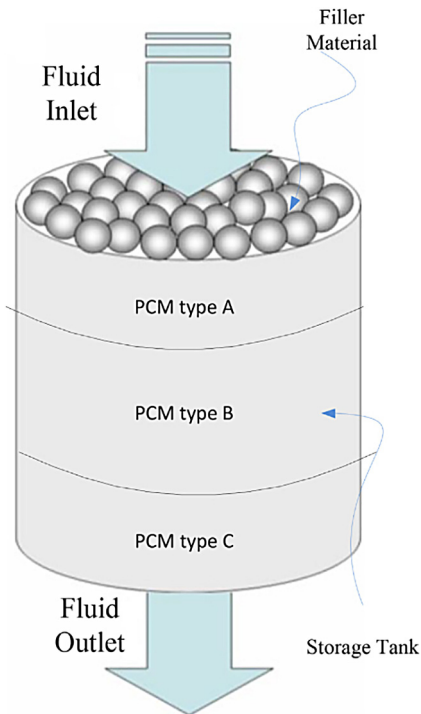


Fig. 34. Sketch of the CLHS system (Shamsi et al., 2017).

concept for CSP plants which goals to avoid the performance degradation through time of traditional thermocline storage. The new concept consists of different solid filler materials and encapsulated PCM inside a multi-layer storage tank where molten salts act as HTF. To simulate the thermocline-tank the following assumptions were considered: 1D fluid flow and temperature distribution and 1D heat transfer in filler spherical capsules; constant density of solid and PCM; heat in flow direction and between capsules was neglected as well as radiation transfer. To determine the temperatures of the materials the equations were discretized using the Finite Volume Method (FVM). In Fig. 37 the storage tank with discretization details is shown and in Fig. 38 the MLSPCM configuration with the different layers is depicted. A comparison of the performance of the new storage configuration with different thermoclines, single PCM and cascaded PCM was performed via simulations. Some operating conditions were fixed for the comparison. The study showed that the multi-layer solid-PCM storage configuration is a promising solution for TES in CSP Plants.

Galione et al. (2015) continued with the study of the MLSPCM storage configuration. In addition to the study performed in the

previous publications about the individual performance of different storage configurations, also the integration of the PLSPCM configuration a CSP Plant (Andasol 1, Spain) through a numerical model was studied. The performance of the PLSPCM storage tank working with operational conditions of the CSP plant considering sun irradiation variations and thermal influence of tank walls and foundation was simulated. After this study, the authors concluded that the variability of operations conditions affects the performance of TES, being feasible that TES configurations that behave properly when they are studied isolated, do not work so good when they are integrated with the fluctuations of a CSP Plant.

#### 4.2.3. Flat plate configuration

Vogel et al. (2016) presented a numerical model to study the natural convection in high temperature latent heat storage systems with flat plate configuration. The natural convection was studied for different widths and heights of enclosure dimensions studying their correlation. The authors introduced a new factor called convective enhancement factor to study the influence of natural convection in heat transfer enhancement. MATLAB and ANSYS Fluent CFD were used to perform the model. Again the material  $\text{KNO}_3\text{-NaNO}_3$  was selected for this study. The model was validated with an experimental LHS test facility.

#### 4.2.4. Fin and tube configuration

Neumann et al. (2017) presented a mathematical model of latent heat storage system integrated on a fin-and-tubes heat exchanger performed with the software COMSOL. The models consisted of 1D model for the simulation of the tubes and a simplified 3D model for the PCM material and fins. Again convection and volume change in the PCM was neglected. The model was validated with two different systems with different heat exchangers and materials. The model showed good accuracy to calculate the power and the characteristics of the heat exchangers. In Fig. 39 the fin and tube exchanger and the 3D model are shown.

#### 4.2.5. Miscellaneous

Pincemin et al. (2008) studied based on a simulation (and also on experiments) the enhancement of thermal conductivity through the integration of graphite foils in PCM and other composites and compared it with the pure materials. The two main variables of the model were the geometric variation with impact on the storage capacity and the time required for the phase change. The simulated configuration is shown in Fig. 40. According to the simulations, the pure PCM required much larger phase change period as the other configurations. The authors concluded that every particular case would need a different amount of graphite in the composite and different distance between foils.

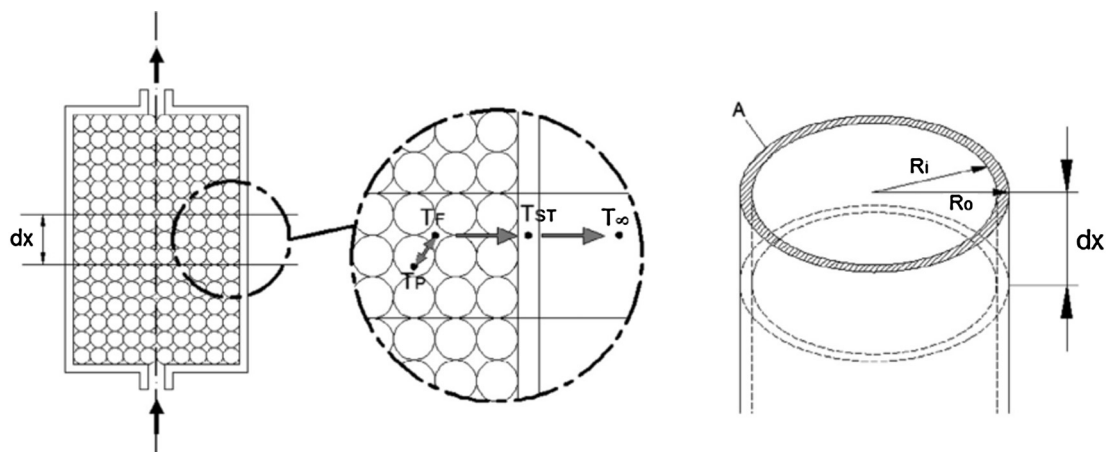


Fig. 35. Longitudinal section (a), heat transfer (b) and vessel cross section (c) (Manfrida et al., 2016).

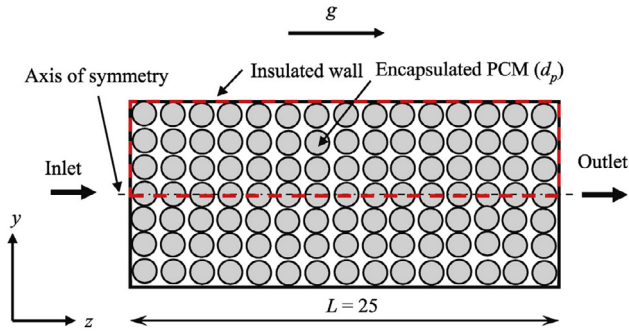


Fig. 36. Scheme of the numerical domain (Bhagat and Saha, 2016).

Pan et al. (2017) presented a novel numerical method called Layered Thermal Resistance (LTR) to optimize the modelling of the solidification process in 1D, 2D and 2D of latent heat thermal storage systems with and without fins. The novel model considers that the solidification temperature ( $T_w$ ) was cooled by constant temperature ( $T_m$ ). The LTR approach was compared with CFD simulations results from simulations based on the solidification and melting model (<https://www.sharcnet.ca/Software/Fluent6/html/ug/node973.htm>). LTR model showed good accuracy regarding solidification time. The finned LTR models consisted in the modelling of the transient nonlinear freezing process of finned PCM. A sketch of the 3D PCM covered by plate fins is shown in Fig. 40.

Zipf (2015) investigated a model for the melting and crystallization of Solar Salt using the Screw-Heat-Exchanger SHE. This model was validated with experimental lab data, also taking into account the dynamically changing layer thickness of crystallized salt on the surface of the SHE, which is limited in growth by the scratching mechanism of the screws. Similarly the lower heat transfer into the solid phase has been taken into account. The heat transfer fluid WT can be a liquid thermal oil or also water/steam. In Fig. 41 mass and enthalpy flows for a node and timestep  $\delta t$  in the SHE model for PCM material and heat transfer fluid WT inside the heat exchanger is shown.

In Zipf et al. (2015) different configurations of solar thermal power plants with direct steam generating collectors using a LHS system with SHE have been modelled using the simulation tool COLSIM (Wittwer, 1999). It could be shown that using the cost estimations for the LHS system the leveled cost of electricity could be lowered using such an approach.

#### 4.3. Enhancement techniques

For the design of a good PCM storage system some important aspects must be considered. In a system with a container filled permanently with PCM the container must have enough volume to assume the volume change during the phase change, as well as be non-corrosive with the storage material. The design must favor thermal conductivity, have enough heat transfer area and be cost-effective. In Fig. 42, the performance enhancement methods for PCM are presented.

The main disadvantage of PCM is their low thermal conductivity. To increase the amount of heat transfer by time, it is possible to increase the thermal conductivity or the heat transfer area among other enhancement techniques. In order to increase the heat transfer area of PCM both fins and capsules can be used. When macro-encapsulation (Fig. 43) is used, PCM is stored inside spherical capsules or tubes which are at the same time are stored inside a container. For the design of the capsules or tubes, the volume increased in the PCM must be considered. Moreover, encapsulation also prevents for segregation and sedimentation (Alva et al., 2017). The other option to increase the transfer surface is metallic fins or extended surfaces. Graphite foil is very suitable for the purpose since it has high thermal conductivity, low density and needs less volume for the same performance compared to steel fins (Alva et al., 2017). For the enhancement of thermal conductivity, one design consists in the integration of layers of highly conductive materials, such as graphite into the PCM (Fig. 43). The layers must be placed in the direction of the heat transfer (Tamme et al., 2008).

Another method to increase the thermal conductivity is the use of heat pipes. Heat pipes have high effective thermal conductivity. Their incorporation into latent heat storage systems enhances the heat transfer between the HTF and the PCM. In Fig. 44 a TESS with the use of heat pipes is shown. The use of an intermediate heat transfer medium which is high conductive is an alternative for increasing the thermal conductivity of PMC (Fig. 44). The concept is based in the reflux evaporation-condensation occurring in the intermediate HTF (Liu et al., 2012). The last method for the enhancement of heat transfer rate is the composite materials. Materials with high thermal conductivity are embedded into the PCM forming the so-called composite materials. Usually graphite, which has not only high thermal conductivity, but also high chemical stability is selected for this technique.

A completely different approach to the low thermal conductivity and the limited heat transfer into solid PCM is the concept of active heat exchangers. Here the PCM material in liquid or solid form (granules, flakes) is transported by a mechanism to the heat exchange area. The screw heat changer concept of Zipf et al. (2013) is a possible technical concept to realize this idea (see also Fig. 25). The heat transfer is enhanced as always the layer of solid material crystallizing on the heat

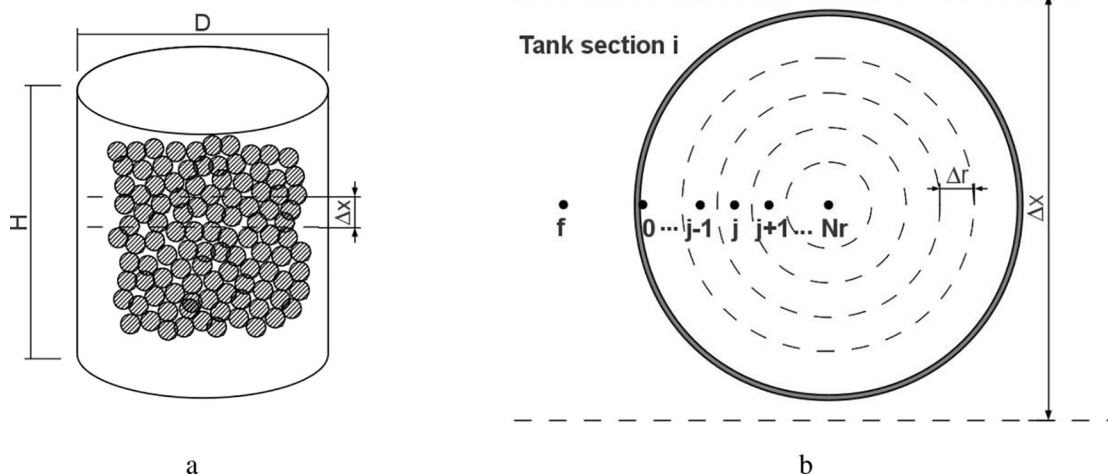


Fig. 37. Cylindrical container with PCM capsules (a); discretization details of the tank (b) (Galione et al., 2014).

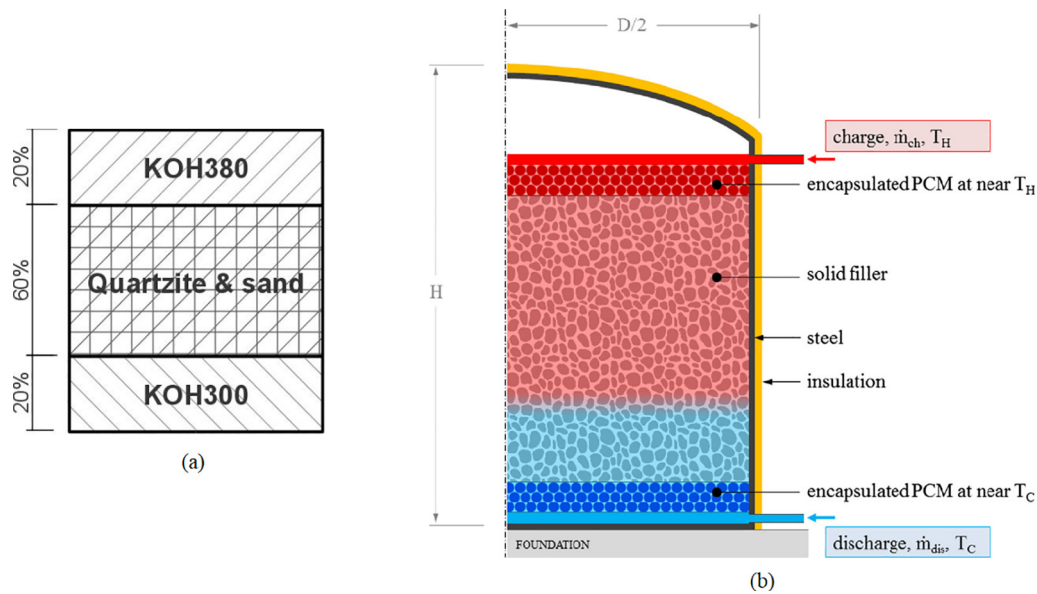


Fig. 38. MLSPCM configuration, KOH380 and KOH300 have high and low melting points respectively (a) (Galione et al., 2014b); Drawing of the PLSPCM tank with three layers (b) (Galione et al., 2015).

exchanger surface is scraped away automatically when reaching a certain thickness.

When just one PCM is used in a TESS, as the HTF transfers the heat to the PCM, the temperature difference between the HTF and the PCM decreases, hence less heat will be transferred over time. For solving this problem storage or multiple PCM method is considered. Different PCMs with different decreasing melting temperatures form the storage system. During the charging process as the HTF flows through the system it will be getting colder, but also the melting temperature of the different PCMs will decrease. Therefore, a nearly constant heat flow to the PCM system will occur. One of the most mentioned publications about cascade latent heat storage (CLHS) was performed by Michels and Pitz-paal (2007). They performed an experimental study based on cascaded LHS with three alkali nitrate salts ( $\text{NaNO}_3$ ,  $\text{KNO}_3$ ,  $\text{KNO}_3/\text{KCl}$ ) using a shell and tube heat exchanger in a medium range of temperatures between 300 and 400 °C. They also performed in the same test module, experiments with single PCM independently. They concluded that CLHS is more advantageous than non-CLHS regarding a higher utilization of the possible phase change and a more uniform outlet temperature over time (Michels and Pitz-paal, 2007). On the other hand, the low conductivity stays as a disadvantage of PCM.

## 5. Conclusions

The heat demand of industrial processes can be supplied by solar energy systems, especially if TES is integrated. Potential industrial

sectors to integrate solar heat are: food industry, brewery industry and chemical industry. The most common range of temperature in thermal industrial processes is below 260 °C. Methods for solar heat integration considering thermal energy storage to optimize the heat use in industrial processes have been presented. Heat integration methodologies, especially for batch processes, are a key factor in the successful and cost-effective use of solar heat together with TES in thermal industrial processes. Nevertheless, the methodologies for optimized integration of thermal energy storage need to be developed further. Latent heat storage systems show very good characteristics for industrial application because they have higher heat storage capacity than sensible TESS, requiring less volume for storing the same amount of energy. Furthermore, they can provide heat at a nearly constant temperature, which is necessary for some thermal industrial applications at medium-high temperatures, such as DSG.

Organic PCMs have higher heat of fusion (134.8–339.8 kJ/kg) in comparison to inorganic materials (20.9–266.1 kJ/kg) within 100–400 °C temperature range but organic PCMs have low thermal conductivity and high-volume change.

On the other hand, inorganic eutectic compositions are the group with more available PCMs for the range of temperatures 120–400 °C. The values of heat of fusion have a range of 74–535 kJ/kg, being higher than for organic and other inorganic substances. The material KOH/LiOH (54/46) reaches the highest value of heat of fusion of the present study with a value of 535 kJ/kg.

Other than heat of fusion and melting point, more information is

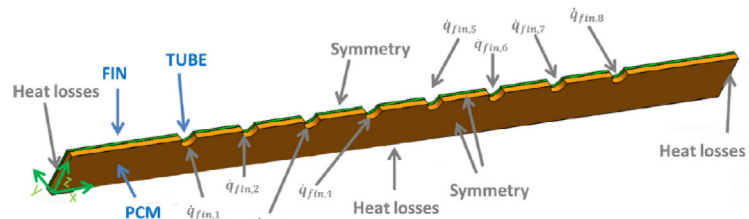
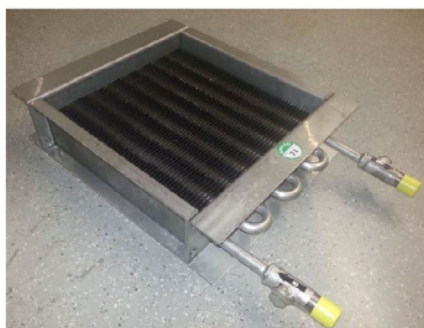


Fig. 39. Fin and tube heat exchanger before adding the PCM; 3D model of the fin including PCM and tubes (Neumann et al., 2017).

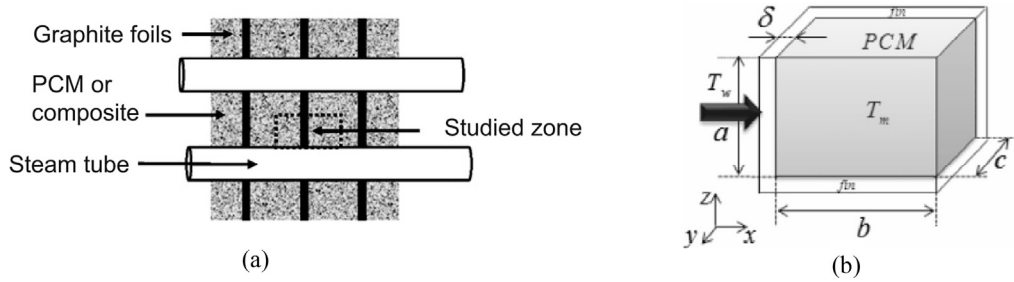


Fig. 40. Simulated configuration (a) (Pincemin et al., 2008); Sketch of a 3D PCM covered by plate fins (b) (Pan et al., 2017).

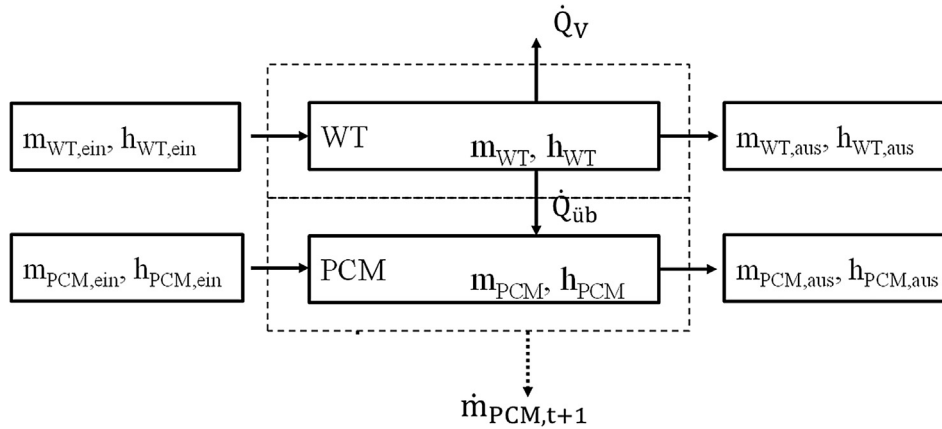


Fig. 41. Mass and enthalpy flows for a node and time-step  $\delta t$  in the SHE model for PCM material and heat transfer fluid WT inside the heat exchanger. Melting process: Molten fluid PCM material  $\dot{m}_{PCM,t+1}$  leaving node;  $\dot{Q}_V$ : heat loss of the heat exchanger to environment;  $\dot{Q}_{ub}$ : heat transferred in heat exchanger to/from PCM.

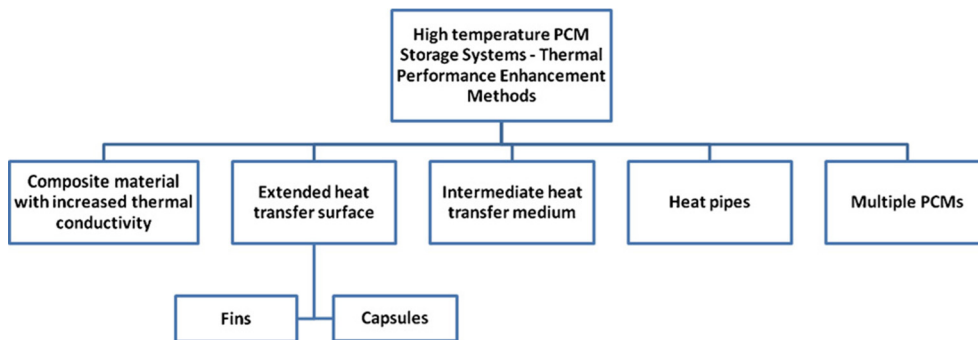


Fig. 42. Different techniques of performance enhancement for PCM (Liu et al., 2012).

necessary in order to perform a comparison between materials considering also charging/discharging properties, subcooling, phase segregation, thermal conductivity and corrosion. Publications about those properties are less common, probably because of the longer time needed for the experiments or because of the higher complexity. Few publications present also information about heat capacity and viscosity of PCMs. However, all these properties are important for the selection of an appropriate PCM and must be further study.

Although several publications regarding experimental set-ups available to test PCMs have been published, still no international or national methodologies have been defined to measure the properties of TES. Most of the experimental set-ups in the range of temperatures 120–400 °C have been designed for direct steam generation, but with the goal of power generation in CSP plants and not for process heat. The most common PCM used in set-ups at the study range of temperatures is

the inorganic salt  $\text{NaNO}_3$  and its eutectic mixtures  $\text{KNO}_3\text{-NaNO}_3$  and  $\text{KNO}_3\text{-NaNO}_2\text{-NaNO}_3$ . More pilot plants for testing PCM integrated with solar-powered thermal industrial processes should be performed. Operation conditions of thermal processes fluctuate in time, therefore specific studies for charging and discharging cycles must be built.

Regarding numerical modelling of TES systems which include PCM, the type of configuration more simulated is the shell and tube configuration, followed by the packed bed configuration. Thereby, the enthalpy method is the methodology more used for the authors to simulate the phase change process of the PCM.

Until now, few LHTES systems have been tested specifically in solar process heat applications. Further experimental set-ups to study the integration of LHTES in thermal industrial processes should be performed in order to test their behavior in the face of different charging/discharging cycles and operational conditions.

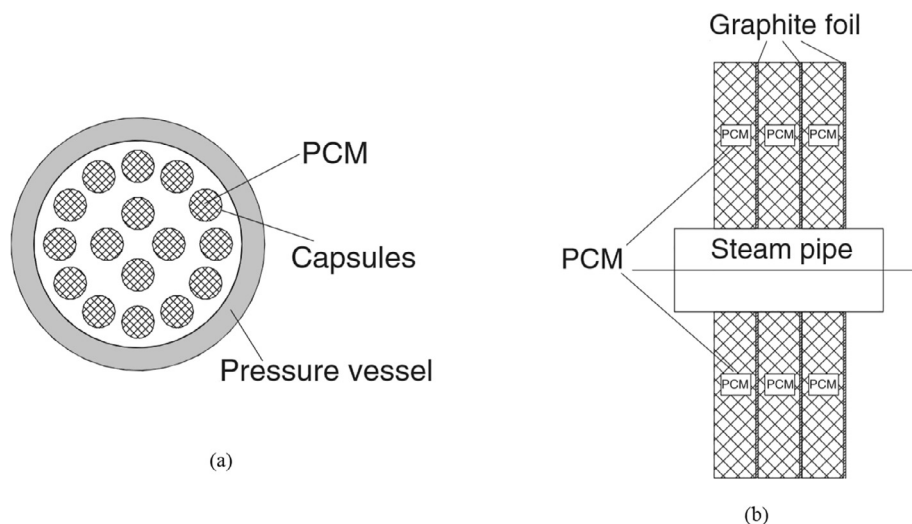


Fig. 43. Macro-encapsulated PCM embedded in a vessel (a) design of PCMs with graphite foil layers (b) (Tamme et al., 2008).

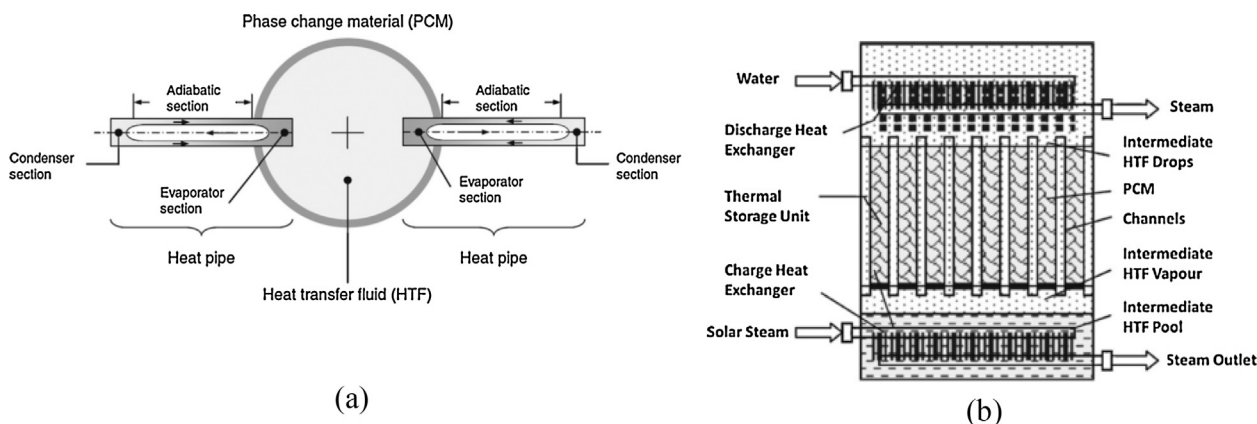


Fig. 44. Heat transfer using heat pipes (a) (Liu et al., 2012); TESS with intermediate heat transfer medium (Liu et al., 2012).

## Acknowledgements

Alicia Crespo, Dr. Mercedes Ibarra and Prof. Dr. Werner Platzer acknowledge the generous financial support provided by CORFO (Corporación de Fomento de la Producción) under the project 13CEI2-21803. Mercedes Ibarra also acknowledges CONICYT/FONDAP/15110019 “Solar Energy Research Center” SERC-Chile.

This work has been partially funded by the European Union’s Horizon 2020 research and innovation programme under the MarieSkłodowska-Curie grant agreement No 712949 (TECNIOspring PLUS) and from the Agency for Business Competitiveness of the Government of Catalonia.

## References

- Abe, Y., Kamimoto, M., Kanari, K., Ozawa, T., Sakamoto, R., Takahashi, Y., 1984. Peak load coverage by molten salts latent thermal storage. In: Proceedings of the 19th Intersociety Energy Conversion Engineering Conference.
- Abhat, A., 1983. Low temperature latent heat thermal energy storage: heat storage materials. *Sol. Energy* 30, 313–332.
- Agyenim, F., Eames, P., Smyth, M., 2011. Experimental study on the melting and solidification behaviour of a medium temperature phase change storage material (Erythritol) system augmented with fins to power a LiBr/H<sub>2</sub>O absorption cooling system. *Renew. Energy* 36, 108–117. <https://doi.org/10.1016/j.renene.2010.06.005>.
- Akiyama, T., Ashizawa, Y., Yagi, J., 1992. Storage and release of heat in a single spherical capsule containing phase-change material with a high melting point. *Heat Transf. Jpn. Res.* 21, 199–217.
- Alva, G., Liu, L., Huang, X., Fang, G., 2017. Thermal energy storage materials and systems for solar energy applications. *Renew. Sustain. Energy Rev.* 68, 693–706. <https://doi.org/10.1016/j.rser.2016.10.021>.
- Atkins, M.J., Walmsley, M.R.W., Neale, J.R., 2010. The challenge of integrating non-continuous processes – milk powder plant case study. *J. Clean. Prod.* 18, 927–934. <https://doi.org/10.1016/j.jclepro.2009.12.008>.
- Atkins, M.J., Walmsley, M.R.W., Morrison, A.S., 2010. Integration of solar thermal for improved energy efficiency in low-temperature-pinch industrial processes. *Energy* 35, 1867–1873. <https://doi.org/10.1016/j.energy.2009.06.039>.
- Atkins, M.J., Walmsley, M.R.W., Neale, J.R., 2012. Process integration between individual plants at a large dairy factory by the application of heat recovery loops and transient stream analysis. *J. Clean. Prod.* 34, 21–28. <https://doi.org/10.1016/j.jclepro.2012.01.026>.
- Babaev, B., 2002. System NaF–NaCl–NaNO<sub>3</sub>. *Inorgan. Mater.* 38 (1), 83–84.
- Barone, G., Della Gatta, G., Ferro, D., Piacente, V., 1990. Enthalpies and entropies of sublimation, vaporization and fusion of 9 polyhydric alcohols. *J. Chem. Soc. Faraday Trans.*
- Barreneche, C.L., Gil, A., Sheth, F., Inés, A., 2013. Fernández, Effect of D-mannitol polymorphism in its thermal energy storage capacity when it is used as PCM. *Sol. Energy* 94, 344–351.
- Bauer, T., Laing, D., Kroner, U., Tamme, R., 2009. Sodium nitrate for high temperature latent heat storage. In: The 11th International Conference on Thermal Energy Storage – Effstock 14–17 June 2009 in Stockholm, Sweden, pp. 1–8.
- Bayón, R., Rojas, E., Valenzuela, L., Zarza, E., León, J., 2010. Analysis of the experimental behaviour of a 100 kWth latent heat storage system for direct steam generation in solar thermal power plants. *Appl. Therm. Eng.* 30, 2643–2651. <https://doi.org/10.1016/j.applthermaleng.2010.07.011>.
- Bellan, S., Gonzalez-Aguilar, J., Archibald, A.R., Romero, M., Rahman, M.M., Goswami, D.Y., Stefanakos, E.K., 2014. Transient numerical analysis of storage tanks based on encapsulated PCMs for heat storage in concentrating solar power plants. *Energy Procedia* 57, 672–681. <https://doi.org/10.1016/j.egypro.2014.10.222>.
- Bhagat, K., Saha, S.K., 2016. Numerical analysis of latent heat thermal energy storage using encapsulated phase change material for solar thermal power plant. *Renew. Energy* 95, 323–336. <https://doi.org/10.1016/j.renene.2016.04.018>.
- Bhale, P.V., Rathod, M.K., Sahoo, L., 2015. Thermal Analysis of a Solar Concentrating System Integrated with Sensible and Latent Heat Storage. *Energy Procedia* 75, 2157–2162. <https://doi.org/10.1016/j.egypro.2015.07.357>.
- Blanco-Rodríguez, P., Rodríguez-Aseguinolaza, J., Risuño, E., Tello, M., 2014.

- Thermophysical characterization of Mg-51Zn eutectic metal alloy: a phase change material for thermal energy storage in direct steam generation applications. *Energy* 72, 414–420. <https://doi.org/10.1016/j.energy.2014.05.058>.
- Brancato, F.A., Frazzica, V., Sapienza, A., 2017. Identification and characterization of promising phase change materials for solar cooling applications. *Sol. Energy Mater. Sol. Cells* 160, 225–232.
- Buschle, J., Steinmann, W.D., Tamme, R., 2006. Analysis of steam storage systems using Modelica. *Aerospace* 235–242.
- Cabeza, L.F., Castell, A., Barreneche, C., de Gracia, A., Fernández, A.I., 2011. Materials used as PCM in thermal energy storage in buildings: a review. *Renew. Sustain. Energy Rev.* 15, 1675–1695. <https://doi.org/10.1016/j.rser.2010.11.018>.
- Cabeza, L.F., Martorell, I., Miró, L., Fernández, I., Barreneche, C., 2015. Introduction to thermal energy storage (TES) systems, Chapter 1, In: Cabeza, L. (Ed.), *Advances in Thermal Energy Storage Systems*. Editor: Woodhead Publishing. ISBN 978-1-78242-088-0.
- Cabeza, L., Mehling, H., 2008. *Heat and Cold Storage with PCM. An Up to Date Introduction Into Basics and Applications*. Springer ISBN:978-3-540-68557-9.
- Cárdenas, B., León, N., 2013. High temperature latent heat thermal energy storage: phase change materials, design considerations and performance enhancement techniques. *Renew. Sustain. Energy Rev.* 27, 724–737. <https://doi.org/10.1016/j.rser.2013.07.028>.
- Chen, C., Ciou, Y., 2009. Design of indirect heat recovery systems with variable temperature storage for batch plants. *Ind. Eng. Chem. Res.* 48, 75–87.
- Cottret N, Menichetti E. Technical study report on solar heat for industrial processes – State of the art in the Mediterranean region. <[http://www.solarthermalworld.org/sites/gstec/files/story/2015-10-14/solar\\_heat\\_for\\_industrial\\_processes\\_technical\\_report\\_state\\_of\\_the\\_art\\_in\\_the\\_mediterranean\\_region.pdf](http://www.solarthermalworld.org/sites/gstec/files/story/2015-10-14/solar_heat_for_industrial_processes_technical_report_state_of_the_art_in_the_mediterranean_region.pdf)> (download date: 04-06-2017).
- Dieckmann, J., Latent heat in concrete, Tec. Univ. Kaiserslautern, Germany. <[http://www.eurosolar.org/new/pdfs\\_neu/Thermal/IRES2006\\_Dieckmann.pdf](http://www.eurosolar.org/new/pdfs_neu/Thermal/IRES2006_Dieckmann.pdf)> (download date: 14-08-2017).
- Eiholzer, T., Olsen, D., Hoffmann, S., Sturm, B., Wellig, B., 2017. Integration of a solar thermal system in a medium-sized brewery using pinch analysis: methodology and case study. *Appl. Therm. Eng.* 113, 1558–1568. <https://doi.org/10.1016/j.applthermaleng.2016.09.124>.
- Fan, Z., Infante Ferreira, C.A., Mosaffa, A.H., 2014. Numerical modelling of high temperature latent heat thermal storage for solar application combining with double-effect H<sub>2</sub>O/LiBr absorption refrigeration system. *Sol. Energy* 110, 398–409. <https://doi.org/10.1016/j.solener.2014.09.036>.
- Farkas, D., Birchenall, C., 1985. New eutectic alloys and their heats of transformation. *Metall. Mater. Trans.* A 16–3, 323–328.
- Fernández, A.I., Barreneche, C., Belusko, M., Segarra, M., Bruno, F., Cabeza, L.F., 2017. Considerations for the use of metal alloys as phase change materials for high temperature applications. *Sol. Energy Mater. Sol. Cells* 171, 275–281. <https://doi.org/10.1016/j.solmat.2017.06.054>.
- Fornarelli, F., Ceglie, V., Fortunato, B., Camporeale, S.M., Torresi, M., Oresta, P., Miliozzi, A., 2017. Numerical simulation of a complete charging-discharging phase of a shell and tube thermal energy storage with phase change material. *Energy Procedia* 126, 501–508. <https://doi.org/10.1016/j.egypro.2017.08.220>.
- Gallione, P.A., Pérez-Segarra, C.D., Rodríguez, I., Lehmkuhl, O., Rigola, J., 2014. A new thermocline-PCM thermal storage concept for CSP plants. Numerical Analysis and Perspectives. *Energy Procedia* 49, 790–799. <https://doi.org/10.1016/j.egypro.2014.03.086>.
- Gallione, P.A., Pérez-Segarra, C.D., Rodríguez, I., Torras, S., Rigola, J., 2015. Multi-layered solid-PCM thermocline thermal storage for CSP. Numerical evaluation of its application in a 50MWe plant. *Sol. Energy* 119, 134–150. <https://doi.org/10.1016/j.solener.2015.06.029>.
- García, P., Olcese, M., Rougé, S., 2015. Experimental and numerical investigation of a pilot scale latent heat thermal energy storage for CSP power plant. *Energy Procedia* 69, 842–849. <https://doi.org/10.1016/j.egypro.2015.03.102>.
- Ge, H., Li, H., Mei, S., Liu, J., 2013. Low melting point liquid metal as a new class of phase change material: an emerging frontier in energy area. *Renew. Sustain. Energy Rev.* 21, 331–346. <https://doi.org/10.1016/j.rser.2013.01.008>.
- Gil, A., Medrano, M., Martorell, I., Lázaro, A., Dolado, P., Zalba, B., Cabeza, L.F., 2010. State of the art on high temperature thermal energy storage for power generation. Part 1-Concepts, materials and modellization. *Renew. Sustain. Energy Rev.* 14, 31–55. <https://doi.org/10.1016/j.rser.2009.07.035>.
- Gil, A., Oró, E., Peiró, G., Álvarez, S., Cabeza, L.F., 2013. Material selection and testing for thermal energy storage in solar cooling. *Renew. Energy* 57, 366–371. <https://doi.org/10.1016/j.renene.2013.02.008>.
- Gil, A., Barreneche, C., Moreno, P., Solé, C., Inés Fernández, A., Cabeza, L.F., 2013. Thermal behaviour of d-mannitol when used as PCM: Comparison of results obtained by DSC and in a thermal energy storage unit at pilot plant scale. *Appl. Energy* 111, 1107–1113. <https://doi.org/10.1016/j.apenergy.2013.04.081>.
- Gimenez-Gavarrell, P., Fereres, S., 2017. Glass encapsulated phase change materials for high temperature thermal energy storage. *Renew. Energy* 107, 497–507. <https://doi.org/10.1016/j.renene.2017.02.005>.
- Guo, C., Zhang, W., 2008. Numerical simulation and parametric study on new type of high temperature latent heat thermal energy storage system. *Energy Convers. Manage.* 49, 919–927. <https://doi.org/10.1016/j.enconman.2007.10.025>.
- Hailiot, D., Bauer, T., Kröner, U., Tamme, R., 2011. Thermal analysis of phase change materials in the temperature range 120–150 °C. *Thermochim. Acta* 513, 49–59. <https://doi.org/10.1016/j.tca.2010.11.011>.
- Heller, L., 2013. Literature Review on Heat Transfer Fluids and Thermal Energy Storage Systems in CSP Plants – STERG Report, <[http://www.solarthermalworld.org/uploads/2011/08/HTF\\_TESmed\\_Review\\_2013\\_05\\_311.pdf](http://www.solarthermalworld.org/uploads/2011/08/HTF_TESmed_Review_2013_05_311.pdf)> (download date: 15.05.2017).
- Herrmann, U., Geyer, M., Kearney, D., 2002. Overview on Thermal Storage Systems – Workshop on Thermal Storage for Trough Power Systems – FLABEG Solar International GmbH. <[https://energjalatgud.ee/img\\_auth.php/f/f/Herrmann%2CU.%2CGeyer%2CM.%2CKearney%2CD.FLABEG.Solar.Int.GmbH.Overview\\_of\\_thermal\\_storage\\_systems\\_2002.pdf](https://energjalatgud.ee/img_auth.php/f/f/Herrmann%2CU.%2CGeyer%2CM.%2CKearney%2CD.FLABEG.Solar.Int.GmbH.Overview_of_thermal_storage_systems_2002.pdf)> (download date: 28-10-2017).
- Hoshi, A., Mills, D.R., Bittar, A., Saitoh, T.S., 2005. Screening of high melting point phase change materials (PCM) in solar thermal concentrating technology based on CLFR. *Sol. Energy* 79, 332–339. <https://doi.org/10.1016/j.solener.2004.04.023>.
- Huang, K., Feng, G., Zhang, J., 2014. Experimental and numerical study on phase change material floor in solar water heating system with a new design. *Sol. Energy* 105, 126–138.
- Iwamoto, Y., Ikai, S., 2000. New polymeric material for latent heat thermal energy storage. In: 5th Workshop of the IEA ECES IA Annex 10, Tsu (Japan).
- Jabbar, A., Khalifa, N., Suffer, K., Mahmoud, M., 2013. A storage domestic solar hot water system with a back layer of phase change material. *Exp. Therm. Fluid Sci.* 44, 174–181.
- Jaguemont, J., Omar, N., Van den Bossche, P., Mierlo, J., 2018. Phase-change materials (PCM) for automotive applications: a review. *Appl. Therm. Eng.* 132, 308–320. <https://doi.org/10.1016/j.applthermaleng.2017.12.097>.
- Joemann, M., Oezcan, T., Kauffeld, M., Pollerberg, C., 2016. Process steam and chilled water production with CPC-collectors, steam jet ejector chiller and latent heat storages. *Energy Procedia* 91, 767–776. <https://doi.org/10.1016/j.egypro.2016.06.242>.
- Johnson, M., Fiss, M., Klemm, T., Eck, M., 2014. Test and analysis of a flat plate latent heat storage design. *Energy Procedia* 57, 662–671. <https://doi.org/10.1016/j.egypro.2014.10.221>.
- Kakiuchi, H., Yamayaki, M., Yabe, M., Chihara, S., Terunuma, Y., Sakata, Y., Usami, T., 1998. A study of erythritol as phase change material. In: 2nd Workshop of the IEA ECES IA Annex 10, Sofia (Bulgaria).
- Kalogirou, S., 2003. The potential of solar industrial process heat applications. *Appl. Energy* 76, 337–361. [https://doi.org/10.1016/S0306-2619\(02\)00176-9](https://doi.org/10.1016/S0306-2619(02)00176-9).
- Kamimoto, M., Abe, Y., Sawata, S., Tani, T., Ozawa, T., 1985. Latent heat storage unit using form-stable high density polyethylene for solar thermal applications. In: Proceedings of the International Symposium on Thermal Application of Solar Energy, Hakone (Kanagawa, Japan).
- Kemp, I.C., Deakin, A.W., 1989. Cascade analysis for energy and process integration of batch processes. Part 1. Calculation of energy targets. *Chem. Eng. Res. Des.* 67, 495–509.
- Kemp, I.C., 2007. *Pinch Analysis and Process Integration – Institution of Chemical Engineering – Editors: Butterworth-Heinemann, second ed.* ISBN: 0 7506 8260 4.
- Kenisarin, M.M., 1993. Short-term storage of solar energy 1. Low temperature phase-change materials. *Appl Sol. Energy*.
- Kenisarin, M.M., 2010. High-temperature phase change materials for thermal energy storage. *Renew. Sustain. Energy Rev.* 14, 955–970. <https://doi.org/10.1016/j.rser.2009.11.011>.
- Kenisarin, M., Mahkamov, K., 2007. Solar energy storage using phase change materials. *Renew. Sustain. Energy Rev.* 11, 1913–1965. <https://doi.org/10.1016/j.rser.2006.05.005>.
- Khan, M.M.A., Saidur, R., Al-Sulaiman, F.A., 2017. A review for phase change materials (PCMs) in solar absorption refrigeration systems. *Renew. Sustain. Energy Rev.* 76, 105–137. <https://doi.org/10.1016/j.rser.2017.03.070>.
- Klemes, J.J., 2013. *Handbook of Process Integration – Minimisation of Energy and Water Use, Waste and Emissions – published by Woodhead Publishing.* ISBN: 978-0-85709-593-0.
- Krummenacher, Pierre, Muster, Bettina, 2015. Methodologies and Software Tools for Integrating Solar Heat Into Industrial Processes. IEA SHC Task 49. <[http://task49.iea-shc.org/data/sites/1/publications/IEATask49.DeliverableB1\\_201502181.pdf](http://task49.iea-shc.org/data/sites/1/publications/IEATask49.DeliverableB1_201502181.pdf)> (download date: 14-06-2017).
- Krummenacher, P., Favrat, D., 2001. Indirect and mixed direct-indirect heat integration of batch processes based on Pinch analysis. *Int. J. Appl. Thermodyn.* 4, 135–143.
- Kurup, P., Turchi, C., 2015. Initial Investigation into the Potential of CSP Industrial Process Heat for the Southwest United States Initial Investigation into the Potential of CSP Industrial Process Heat for the Southwest United States. <<https://www.nrel.gov/docs/fy16osti/64709.pdf>> (download date: 30.05.2017).
- Laing, D., Bahl, C., Baue, T., Lehmann, D., Steinmann, W., 2011. Thermal energy storage for direct steam generation. *Sol. Energy* 85, 627–633.
- Lauterbach, C., Schmitt, B., Vajen, K., 2014. System analysis of a low-temperature solar process heat system. *Sol. Energy* 101, 117–130. <https://doi.org/10.1016/j.solener.2013.12.014>.
- Li, Q., Tehrani, S.S.M., Taylor, R.A., 2017. Techno-economic analysis of a concentrating solar collector with built-in shell and tube latent heat thermal energy storage. *Energy* 121, 220–237. <https://doi.org/10.1016/j.energy.2017.01.023>.
- Linnhoff, B., Ashton, G.J., Obeng, E.D.A., 1988. Process integration of batch processes. In: *Underst. Process Integr. II E IChemE. Hemisph. Publ. Corp.*, pp. 221–238.
- Liu, M., Saman, W., Bruno, F., 2012. Review on storage materials and thermal performance enhancement techniques for high temperature phase change thermal storage systems. *Renew. Sustain. Energy Rev.* 16, 2118–2132. <https://doi.org/10.1016/j.rser.2012.01.020>.
- Mahfuz, M.H., Anisur, M.R., Kibria, M.A., Saidur, R., Metselaar, I.H.S.C., 2014. Performance investigation of thermal energy storage system with phase change material (PCM) for solar water heating application. *Int. Commun. Heat Mass Transf.* 57, 132–139.
- Manfrida, G., Sechi, R., Stańczyk, K., 2016. Modelling and simulation of phase change material latent heat storages applied to a solar-powered Organic Rankine Cycle. *Appl. Energy* 179, 378–388. <https://doi.org/10.1016/j.apenergy.2016.06.135>.

- Medrano, M., Gil, A., Martorell, I., Potau, X., Cabeza, L.F., 2010. State of the art on high-temperature thermal energy storage for power generation. Part 2-Case studies. *Renew. Sustain. Energy Rev.* 14, 56–72. <https://doi.org/10.1016/j.rser.2009.07.036>.
- Michels, H., Pitz-paal, R., 2007. Cascaded latent heat storage for parabolic trough solar power plants. *Sol. Energy* 81, 829–837. <https://doi.org/10.1016/j.solener.2006.09.008>.
- Morisson, V., Rady, M., Palomo, E., Arquies, E., 2008. Thermal energy storage systems for electricity production using solar energy direct steam generation technology. *Chem. Eng. Process. Process. Intensif.* 47, 499–507. <https://doi.org/10.1016/j.ccep.2007.01.025>.
- Muren, R., Arias, D., Luptowski, B., 2009. Performance based cost modelling of phase change thermal energy storage for high temperature concentrating solar power systems. In: ASME 2009 Int. Mech. Eng. Congr. Expo.
- Muster, B., Ben Hassine, I., Helmke, A., Heß, S., Krummenacher, P., Schmitt, B., Schnitzer, H., 2015. Integration Guideline, IEA SHC Task 49HC Task 49 – Deliv. B2. 99. [http://task49.iea-shc.org/data/sites/1/publications/150218\\_IEATask49\\_D\\_B2\\_IntegrationGuideline-final1.pdf](http://task49.iea-shc.org/data/sites/1/publications/150218_IEATask49_D_B2_IntegrationGuideline-final1.pdf).
- Nallusamy, N., Velraj, R., 2009. Numerical and experimental investigation on a combined sensible and latent heat storage unit integrated with solar water heating system. *J. Sol. Energy Eng.* 131, 41002. <https://doi.org/10.1115/1.3197600>.
- Nallusamy, N., Sampath, S., Velraj, R., 2007. Experimental investigation on a combined sensible and latent heat storage system integrated with constant/varying (solar) heat sources. *Renew. Energy* 32, 1206–1227. <https://doi.org/10.1016/j.renene.2006.04.015>.
- Neumann, H., Palomba, V., Frazzica, A., Seiler, D., Wittstadt, U., Gschwander, S., Restuccia, G., 2017. A simplified approach for modelling latent heat storages: application and validation on two different fin-and-tubes heat exchangers. *Appl. Therm. Eng.* 125, 41–52. <https://doi.org/10.1016/j.applthermaleng.2017.06.142>.
- Niyas, H., Prasad, S., Muthukumar, P., 2017. Performance investigation of a lab-scale latent heat storage prototype—numerical results. *Energy Convers. Manage.* 135, 188–199. <https://doi.org/10.1016/j.enconman.2016.12.075>.
- Nomura, T., Okinaka, N., Akiyama, T., 2010. Waste heat transportation system, using phase change material (PCM) from steelworks to chemical plant. *Resour. Conserv. Recycl.* 54, 1000–1006.
- Nomura, T., Oya, T., Okinaka, N., Akiyama, T., 2010. Feasibility of an advanced waste heat transportation system using high-temperature phase change material (PCM). *ISIJ Int.* 50, 1326–1332.
- Pan, C., Hoenig, S., Chen, C.-H., Neti, S., Romero, C., Vermaak, N., 2017. Efficient melting of phase change material solidification with multidimensional fins. *Int. J. Heat Mass Transf.* 115, 897–909. <https://doi.org/10.1016/j.ijheatmasstransfer.2017.07.120>.
- Philips, W., Stearns, J., 1985. Advanced latent heat of fusion thermal energy storage for solar power systems. In: Proceedings of the 20th Intersociety Energy Conversion Engineering Conference, pp. 384–391.
- Pilkington Solar Int. GmbH, Cologne, Germany. 2000. Survey of Thermal Storage for Parabolic Trough Power Plants, NREL/SR-550-27925 Report. <http://marcellacroix.espaceweb.usherbrooke.ca/ENERGIE/Thermal-storage.pdf> (download date: 10-06-2017).
- Pincemin, S., Olives, R., Py, X., Christ, M., 2008. Highly conductive composites made of phase change materials and graphite for thermal storage. *Sol. Energy Mater. Sol. Cells* 92, 603–613. <https://doi.org/10.1016/j.solmat.2007.11.010>.
- Pintaldi, S., Perfumo, C., Sethuvenkatraman, S., White, S., Rosengarten, G., 2015. A review of thermal energy storage technologies and control approaches for solar cooling. *Renew. Sustain. Energy Rev.* 41, 975–995. <https://doi.org/10.1016/j.rser.2014.08.062>.
- Plataforma Solar de Almería. Informe Anual. 2007. <https://www.psa.es/es/techrep/2007/ATR2007-esp.pdf> (download date: 27-10-2017).
- Pointner, H., Steinmann, W.D., 2016. Experimental demonstration of an active latent heat storage concept. *Appl. Energy* 168, 661–671. <https://doi.org/10.1016/j.apenergy.2016.01.113>.
- Pollerberg, C., Kauffeld, M., Oezcan, T., Koffler, M., Hanu, L.G., Doetsch, C., 2012. Latent heat and cold storage in a solar-driven steam jet ejector chiller plant. *Energy Procedia* 30, 957–966. <https://doi.org/10.1016/j.egypro.2012.11.108>.
- Quijara, J.A., Alriols, M.G., Labidi, J., 2011. Integration of a solar thermal system in a dairy process. *Renew. Energy* 36, 1843–1853. <https://doi.org/10.1016/j.renene.2010.11.029>.
- Quijara, J.A., Garcia, A., Alriols, M.G., Labidi, J., 2013. Heat integration options based on pinch and exergy analyses of a thermosolar and heat pump in a fish tinning industrial process. *Energy* 55, 23–37. <https://doi.org/10.1016/j.energy.2013.02.025>.
- Rodriguez-Garcia, M.M., Bayon, R., Rojas, E., 2016. Stability of D-mannitol upon melting/freezing cycles under controlled inert atmosphere. *Energy Procedia* 91, 218–225. <https://doi.org/10.1016/j.egypro.2016.06.207>.
- Ruiz-Cabañas, F.J., Jové, A., Prieto, C., Madina, V., Fernández, A.I., Cabeza, L.F., 2017. Materials selection of steam-phase change material (PCM) heat exchanger for thermal energy storage systems in direct steam generation facilities. *Sol. Energy Mater. Sol. Cells* 159, 526–535. <https://doi.org/10.1016/j.solmat.2016.10.010>.
- Schroeder, J., 1975. Thermal energy storage and control. *J. Eng. Ind.* 97 (3), 893–896.
- Schweiger, H., Mendes, J.F., Benz, N., Hennecke, K., Prieto, G., Cusi, M., Gonçalves, H., 2000. The potential of solar heat in industrial processes. In: A State of the Art Review for Spain and Portugal, Conf. Eurosun, Copenhagen.
- Shamsi, H., Boroushaki, M., Geraei, H., 2017. Performance evaluation and optimization of encapsulated cascade PCM thermal storage. *J. Energy Storage* 11, 64–75. <https://doi.org/10.1016/j.est.2017.02.003>.
- Sharma, R.K., Ganesan, P., Tyagi, V.V., Metselaar, H.S.C., Sandaran, S.C., 2015. Developments in organic solid–liquid phase change materials and their applications in thermal energy storage. *Energy Convers. Manage.* 95, 193–228. <https://doi.org/10.1016/j.enconman.2015.01.084>.
- Sharma, S.D., Sagara, K., 2013. Latent heat storage materials and systems: a review. *Int. J. Green Energy* 37–41. <https://doi.org/10.1081/GE-200051299>.
- Shin, B.C., Kim, S.D., 1990. Ternary carbonate eutectic (lithium, sodium and potassium carbonates for latent heat storage medium. *Sol. Energy* 21, 81–90.
- Solar Heat for Industry – Solar Payback, 2017. <https://www.solar-payback.com/wp-content/uploads/2017/07/Solar-Heat-for-Industry-Solar-Payback-April-2017.pdf> (download date: 14.06.2017).
- Solé, A., Neumann, H., Niedermaier, S., Martorell, I., Schossig, P., Cabeza, L.F., 2014. Stability of sugar alcohols as PCM for thermal energy storage. *Sol. Energy Mater. Sol. Cells* 126, 125–134.
- Steinmann, W.-D., Tammé, R., 2008. Latent heat storage for solar steam systems. *J. Sol. Energy Eng.* <https://doi.org/10.1115/1.2804624>.
- Stückle, A., Modelling of high temperature storage systems for latent heat. In: 7th Model. Conf., pp. 502–506. <http://doi.org/10.3384/ecp09430031>.
- Tammé, R., Bauer, T., Buschle, J., Laing, D., Steinmann, W., 2008. Latent heat storage above 120 °C for applications in the industrial process heat sector and solar power generation. *Energy Res.* 32, 264–271. <https://doi.org/10.1002/er>.
- Trp, A., 2005. An experimental and numerical investigation of heat transfer during technical grade paraffin melting and solidification in a shell-and-tube latent thermal energy storage unit. In: *Sol. Energy*, Pergamon, pp. 648–660. <http://doi.org/10.1016/j.solener.2005.03.006>.
- Vannoni, C., Riccardo, B., Serena, D., 2008. Potential for Solar Heat in Industrial Processes. Department of Mechanics and Aeronautics - University of Rome "La Sapienza", IEA SHC Task 33 and Solar Paces Task IV: Solar Heat for Industrial Processes. <http://www.aee-intec.at/Uploads/dateien561.pdf> (download date: 15.07.2017).
- Venkatesetty, H., LeFrois, R., 1976. Thermal energy storage for solar power plants. In: Proc. 11th Intersoc. Energy Convers. Eng. Conf., pp. 606–612.
- Vogel, J., Felbinger, J., Johnson, M., 2016. Natural convection in high temperature flat plate latent heat thermal energy storage systems. *Appl. Energy* 184, 184–196. <https://doi.org/10.1016/j.apenergy.2016.10.001>.
- Walmsley, M.R.W., Walmsley, T.G., Atkins, M.J., Neale, J.R., 2012. Area targeting and storage temperature selection for heat recovery loops. *Chem. Eng. Trans.* 29, 1219–1224. <https://doi.org/10.3303/CET1229204>.
- Walmsley, T.G., Walmsley, M.R.W., Atkins, M.J., Neale, J.R., 2014. Integration of industrial solar and gaseous waste heat into heat recovery loops using constant and variable temperature storage. *Energy* 75, 53–67. <https://doi.org/10.1016/j.energy.2014.01.103>.
- Willwerth, L., Rodriguez, M., Rojas, E., Ben Cheikh, R., Jmili, A., Baba, A., Soares, J., Parise, F., Weinzierl, B., Krüger, D., 2017. Commissioning and Tests of a Mini CSP Plant, SolarPaces [http://www.reelcoop.com/admin/content/news/p3\\_solarpaces2017\\_en\\_1503832711.pdf](http://www.reelcoop.com/admin/content/news/p3_solarpaces2017_en_1503832711.pdf) (download date: 29-09-2017).
- Wittwer, C., 1999. Simulation von Regelungssystemen in aktiven solarthermischen Anlagen. Technische Universität Karlsruhe.
- Yagi, J., Akiyama, T., 1995. Storage of thermal-energy for effective use of waste heat from industries. *J. Mater. Process. Technol.* 48, 793–804. [https://doi.org/10.1016/0924-0136\(94\)01723-E](https://doi.org/10.1016/0924-0136(94)01723-E).
- Zalba, B., Marín, J.M., Cabeza, L.F., Mehling, H., 2003. Review on thermal energy storage with phase change: materials, heat transfer analysis and applications. *Appl. Therm. Eng.* 23, 251–283.
- Zipf, V., Neuhäuser, A., Willert, D., Nitz, P., Gschwander, S., Platzer, W., 2013. High temperature latent heat storage with a screw heat exchanger: design of prototype. *Appl. Energy* 109, 462–469. <https://doi.org/10.1016/j.apenergy.2012.11.044>.
- Zipf, V., Neuhäuser, A., Bachelier, C., Leithner, R., Platzer, W., 2015. Assessment of different PCM storage configurations in a 50 MWel CSP plant with screw heat exchangers in a combined sensible and latent storage – simulation results. *Energy Procedia* 1078–1088. <https://doi.org/10.1016/j.egypro.2015.03.215>.
- Zipf, V., 2015. Schneckenwärmeübertrager in Latentwärmespeichersystemen – Tests und Wirtschaftlichkeitsstudie für solarthermische Anlagen Schneckenwärmeübertrager in. Technische Universität Braunschweig.